

**DEVELOPMENT OF A TSUNAMI FORECAST  
MODEL FOR  
PALM BEACH, FLORIDA, USA**

Edison Gica

May 24, 2011

## Table of Contents

List of Tables.....	iii
List of Figures .....	iv
Abstract.....	2
1.0 Background and Objectives .....	2
2.0 Forecast Methodology.....	3
3. Model Development .....	4
3.1 Forecast area .....	5
3.2 Historical events and data .....	6
3.3 Model setup.....	6
4. Results and Discussion .....	8
4.1 Model validation .....	8
4.2 Model stability and reliability.....	8
4.3 Results of tested events.....	9
5. Summary and Conclusion .....	10
6.0 Acknowledgments .....	10
7.0 References .....	11
Appendix A. MOST code *.in file.....	30
A1. Reference model *.in file for Palm Beach, Florida.....	30
A2. Forecast model *.in file for Palm Beach, Florida .....	30
Appendix B. Propagation Database: Atlantic Ocean Unit Sources.....	31
Appendix C. Forecast Model tests in SIFT system. ....	40
C.1 Testing Procedure.....	40
C.2 Results .....	41

## List of Tables

Table 1. MOST setup parameters for reference and forecast models for Palm Beach, Florida. ....	1
Table 2. Grid extents used to determine the final A-grid size in the development of a forecast model and high resolution model. ....	2
Table 3. Synthetic tsunamis tested for Palm Beach, Florida. ....	2
Table 4. Earthquake parameter for unit sources in Atlantic. ....	32
Table 5. Earthquake parameters for unit sources in South Sandwich.....	39
Table 6. Table of maximum and minimum amplitudes (cm) at the Palm Beach, Florida warning point for synthetic and historical events tested using SIFT 3.2 and obtained during development. ....	43

## List of Figures

Figure 1. Google map image of Palm Beach, Florida with location of the inlet into the Intercoastal waterways and the three bridges (Flagler Memorial Bridge, Royal Park Bridge and E State Road 80) that connects the town to West Palm Beach on the western side. ....	3
Figure 2. Plot of 1/3 arc-sec DEM developed by NGDC and used in the development of the forecast model. ....	4
Figure 3. Plot of C-grid extent used in the development of the forecast model. The plot is based on a 1/3 arc-sec DEM developed by NGDC and also indicates the location of tide gauges in the region (Lake Worth Pier and Port of West Palm Beach). The tide gauge at Port of West Palm Beach was removed on October 20, 2010 (Tides and Currents). ....	5
Figure 4. Plot of C-grid extent used in the development of the forecast model indicating cities and towns that are included. ....	6
Figure 5. Google map image showing the existence of the wide continental shelf and islands in the Bahamas relative to the location of Palm Beach, Florida. ....	7
Figure 6. Plots of grid extent used to determine the final A-grid size in the development of a forecast model and high resolution model; top) Largest grid the covers a significant portion of the deep ocean, middle) medium size grid that still covers deep ocean, bottom) smallest grid the is on the continental shelf. ....	8
Figure 7. Location of a synthetic scenario ( $M_w=9.5$ ), relative to Palm Beach, Florida, used to test the domain size. ....	9
Figure 8. Location of points where time series are compared for testing different domain sizes (see Figure 7). ....	10
Figure 9. Comparison of time series plots (top) and maximum tsunami wave amplitude distribution (bottom-left-large domain, bottom-middle-medium domain and bottom-right small domain). The bottom plots of large domain (bottom-left) and medium domain (bottom-middle) are adjusted to match that of the small domain (bottom-right) for consistency. ....	11

Figure 10. Plot of DEM used for the high resolution model; left) A- grid using a grid resolution of 9 arc-sec with the box indicating the location of B-grid, middle) B-grid using a grid resolution of 6 arc-sec with the box indicating the location of C-grid; right) C-grid using a grid resolution of 2/3 arc-seconds. .... 12

Figure 11. Plot of DEM used for the high resolution model; left) A- grid using a grid resolution of 18 arc-sec with the box indicating the location of B-grid, middle) B-grid using a grid resolution of 9 arc-sec with the box indicating the location of C-grid; right) C-grid using a grid resolution of 2 arc-seconds. .... 12

Figure 12. Plot locating the scenarios (Mw=9.4, Mw=7.5, Mw=~0 and 1755 Lisbon) used for testing the stability and reliability of the forecast model and high resolution model in relation to the location of Palm Beach, Florida. .... 13

Figure 13. Time series comparison at Lake Worth Pier tide gauge between the forecast model and high resolution model for 1755 Lisbon and synthetic mega-events with Mw=9.4. Plot shows an almost perfect comparison with very slight variation for sssz01-10 and 1755 Lisbon. .... 14

Figure 14. Plot of maximum tsunami wave amplitude distribution [left), A-grid; middle) B-grid and right) C-grid] and time series [bottom) at Lake Worth Pier tide gauge] for the 1755 Lisbon tsunami using high resolution model. .... 15

Figure 15. Plot of maximum tsunami wave amplitude distribution [left), A-grid; middle) B-grid and right) C-grid] and time series [bottom) at Lake Worth Pier tide gauge] for the 1755 Lisbon tsunami using forecast model. .... 16

Figure 16. Plot of maximum tsunami wave amplitude distribution [left), A-grid; middle) B-grid and right) C-grid] and time series [bottom) at Lake Worth Pier tide gauge] for mega-event (Mw=9.4) case ATSZ38-47AB using high resolution model. .... 17

Figure 17. Plot of maximum tsunami wave amplitude distribution [a), A-grid; b) B-grid and c) C-grid] and time series [d) at Lake Worth Pier tide gauge] for mega-event (Mw=9.4) case ATSZ38-47AB using forecast model. .... 18

Figure 18. Plot of maximum tsunami wave amplitude distribution [left), A-grid; middle) B-grid and right) C-grid] and time series [bottom) at Lake Worth Pier tide gauge] for mega-event (Mw=9.4) case ATSZ48-57AB using high resolution model. .... 19

Figure 19. Plot of maximum tsunami wave amplitude distribution [left), A-grid; middle) B-grid and right) C-grid] and time series [bottom) at Lake Worth Pier tide gauge] for mega-event (Mw=9.4) case ATSZ48-57AB using forecast model. .... 20

Figure 20. Plot of maximum tsunami wave amplitude distribution [left), A-grid; middle) B-grid and right) C-grid] and time series [bottom) at Lake Worth Pier tide gauge] for mega-event (Mw=9.4) case ATSZ58-67AB using high resolution model. ....	21
Figure 21. Plot of maximum tsunami wave amplitude distribution [left), A-grid; middle) B-grid and right) C-grid] and time series [bottom) at Lake Worth Pier tide gauge] for mega-event (Mw=9.4) case ATSZ58-67AB using forecast model. ....	22
Figure 22. Plot of maximum tsunami wave amplitude distribution [left), A-grid; middle) B-grid and right) C-grid] and time series [bottom) at Lake Worth Pier tide gauge] for mega-event (Mw=9.4) case ATSZ68-77AB using high resolution model. ....	23
Figure 23. Plot of maximum tsunami wave amplitude distribution [left), A-grid; middle) B-grid and right) C-grid] and time series [bottom) at Lake Worth Pier tide gauge] for mega-event (Mw=9.4) case ATSZ68-77AB using forecast model. ....	24
Figure 24. Plot of maximum tsunami wave amplitude distribution [left), A-grid; middle) B-grid and right) C-grid] and time series [bottom) at Lake Worth Pier tide gauge] for mega-event (Mw=9.4) case ATSZ82-91AB using high resolution model. ....	25
Figure 25. Plot of maximum tsunami wave amplitude distribution [left), A-grid; middle) B-grid and right) C-grid] and time series [bottom) at Lake Worth Pier tide gauge] for mega-event (Mw=9.4) case ATSZ82-91AB using forecast model. ....	26
Figure 26. Plot of maximum tsunami wave amplitude distribution [left), A-grid; middle) B-grid and right) C-grid] and time series [bottom) at Lake Worth Pier tide gauge] for mega-event (Mw=9.4) case SSSZ01-10AB using high resolution model. ....	27
Figure 27. Plot of maximum tsunami wave amplitude distribution [left), A-grid; middle) B-grid and right) C-grid] and time series [bottom) at Lake Worth Pier tide gauge] for mega-event (Mw=9.4) case SSSZ01-10AB using forecast model. ....	28
Figure 28. Google map plot of northern part of Singer Island showing the water passage way. ....	29
Figure 29. Atlantic Source Zone unit sources. ....	31
Figure 30. South Sandwich Source Zone unit sources. ....	38
Figure 31. Response of the Palm Beach forecast model to synthetic scenario ATSZ 38-47 (alpha=30). Maximum sea surface elevation for a) A-grid, b) B-grid, c) C-grid. Sea surface elevation time series at the C-grid warning point (d). The lower time series plot is	

the result obtained during model development and is shown for comparison with test results. .... 1

Figure 32 Response of the Palm Beach forecast model to synthetic scenario ATSZ 48-57 (alpha=30). Maximum sea surface elevation for a) A-grid, b) B-grid, c) C-grid. Sea surface elevation time series at the C-grid warning point (d). The lower time series plot is the result obtained during model development and is shown for comparison with test results. .... 2

Figure 33. Response of the Palm Beach forecast model to synthetic scenario SSSZ 01-10 (alpha=30). Maximum sea surface elevation for (a) A-grid, b) B-grid, c) C-grid. Sea surface elevation time series at the C-grid warning point (d). The lower time series plot is the result obtained during model development and is shown for comparison with test results. .... 3

# **Development of a Tsunami Forecast Model for Palm Beach, Florida, USA**

**Edison Gica**

## Abstract

The National Oceanic and Atmospheric Administration has developed a tsunami forecast model for Palm Beach, Florida, as part of an effort to provide tsunami forecasts for United States coastal communities. Development, validation, and stability testing of the tsunami forecast model has been conducted to ensure model robustness and stability. The Palm Beach, Florida tsunami forecast model employs the optimized version of the Method of Splitting Tsunami numerical code and the stability and reliability was tested by simulating artificial tsunamis from different source regions. A total of 6 synthetic mega tsunami,  $M_w = 9.4$  events, 1  $M_w = 7.5$  and 1  $M_w = \sim 0$  were used and the forecast model was stable for 24 hours. The Palm Beach, Florida forecast model can generate 4 hours of tsunami wave characteristics in approximately 9.7 minutes of CPU time.

## 1.0 Background and Objectives

The National Oceanic and Atmospheric Administration (NOAA) Center for Tsunami Research (NCTR) at the NOAA Pacific Marine Environmental Laboratory (PMEL) has developed a tsunami forecasting capability for operational use by NOAA's two Tsunami Warning Centers located in Hawai'i and Alaska (Titov *et al.*, 2005). The system is designed to efficiently provide basin-wide warning of approaching tsunami waves accurately and quickly. The system, termed Short-term Inundation Forecast of Tsunamis (SIFT), combines real-time tsunami event data with numerical models to produce estimates of tsunami wave arrival times and amplitudes at a coastal community of interest. The SIFT system integrates several key components: deep-ocean observations of tsunamis in real time, a basin-wide pre-computed propagation database of water level and flow velocities based on potential seismic unit sources, an inversion algorithm to refine the tsunami source based on deep-ocean observations during an event, and high-resolution tsunami forecast models termed Forecast Models.

This report details the development of a tsunami forecast model for Palm Beach, Florida. Development includes construction of a digital elevation model based on available bathymetric and topographic data, model validation with historic events, and stability tests of the model with a suite of mega tsunami events originating from subduction zones in the Atlantic Ocean. Palm Beach, Florida is a 16 mile long barrier island with its eastern side facing the Atlantic Ocean and connected with three bridges (Flagler Memorial Bridge, Royal Park Bridge and E State Road 80) east of the Intracoastal Waterway and West Palm Beach (Figure 1). The town of Palm Beach is not only the wealthiest community in Florida but is considered as one of the most affluent in the entire United States (Delta Skyway Magazine, Dec 2010). The geographical location of Palm Beach is closest to the Gulf Stream thus creating an outstanding marine environment, with lush gardens and palm lined beaches. Palm Beach got its name from a shipwreck named 'Providencia' in January 1878. The ship was loaded with cocoanuts which were bound from Havana to Barcelona. In an effort to launch a tropical South Florida into a commercial cocoanut industry, the early settlers salvage and planted the cocoanuts which were not native to South Florida (Government of Palm Beach).

The town of Palm Beach was incorporated into Palm Beach County, Florida in April 17, 1911. The county was established on July 1, 1909 and is Florida's 47<sup>th</sup> County (Government of Palm Beach). It was originally part of St. Johns County in 1821 and until its official establishment in 1909 it was part of several counties. And from 1909 to 2009 some parts of Palm Beach County were given to other counties. Palm Beach county is defined by water into six physical zones; Atlantic Ocean, barrier islands, lakes and lagoons, sandy flatlands, swamps or marshes and Lake Okeechobee. Palm Beach County has a very diverse community coming from different parts of the US and the world. In the early 19<sup>th</sup> Century the first settlers started to occupy Palm Beach County and found its wilderness beautiful but also daunting with "millions of mosquitoes to the square inch". When the United States was preparing for possible involvement in World War 2, Palm Beach County was an ideal place to train pilots and testing airplanes due to its temperate climate and flat terrain (Palm Beach County).

The population of Palm Beach County in the 1940 pre-war was 80,000 and almost 115,000 by 1950 and quickly increased from that point on with a current (2010) population 1,320,134 (U.S. Census Bureau 2010). The number one economic driver of Palm Beach County's economy is tourism with 3.62 million visitors staying in hotels in the year 2009. Its production of sweet corn, rice, bell peppers, lettuce, radishes, Chinese vegetables, specialty leaf and celery and sugar cane is ranked first in Florida due to its year-round sunny climate. It is also becoming a recognized leader in aerospace/aviation/engineering industry. Industries like B/E Aerospace, Lockheed Martin and Sikorsky Aircraft Corporation are located in Palm Beach County. In the field of life sciences, it has brought in Scripps Research Institute and Max Planck Society into the region. The region will also become the second-largest supplier of "utility-scale" solar power in the nation when the NextEra's Next Generation Solar Energy Center is completed. It was ranked No. 3 by Forbes list of 'Hotbeds of Tomorrow's Technology'. With affluent towns and leading industries in its region, Palm Beach County is the wealthiest county in Florida with an average per capita personal income of \$58,358 (Delta Skyway Magazine, Dec 2010).

## **2.0 Forecast Methodology**

A high-resolution inundation model was used as the basis for development of a tsunami forecast model to operationally provide an estimate of wave arrival time, wave height, and inundation at Palm Beach, Florida following tsunami generation. All tsunami forecast models are run in real time while a tsunami is propagating across the open ocean. The Palm Beach, Florida model was designed and tested to perform under stringent time constraints given that time is generally the single limiting factor in saving lives and property. The goal of this work is to maximize the length of time that the community of Palm Beach, Florida has to react to a tsunami threat by providing accurate information quickly to emergency managers and other officials responsible for the community and infrastructure.

The general tsunami forecast model, based on the Method of Splitting Tsunami (MOST), is used in the tsunami inundation and forecasting system to provide real-time tsunami forecasts at selected coastal communities. The model runs in minutes while employing high-resolution grids constructed by the National Geophysical Data Center. The Method of Splitting Tsunami (MOST) is a suite of numerical simulation codes capable of

simulating three processes of tsunami evolution: earthquake, transoceanic propagation, and inundation of dry land. The MOST model has been extensively tested against a number of laboratory experiments and benchmarks (Synolakis *et al.*, 2008) and was successfully used for simulations of many historical tsunami events. The main objective of a forecast model is to provide an accurate, yet rapid, estimate of wave arrival time, wave height, and inundation in the minutes following a tsunami event. Titov and González (1997) describe the technical aspects of forecast model development, stability, testing, and robustness, and Tang *et al.*, 2009 provide detailed forecast methodology

A basin-wide database of pre-computed water elevations and flow velocities for unit sources covering worldwide subduction zones has been generated to expedite forecasts (Gica *et al.*, 2008). As the tsunami wave propagates across the ocean and successively reaches tsunameter observation sites, recorded sea level is ingested into the tsunami forecast application in near real-time and incorporated into an inversion algorithm to produce an improved estimate of the tsunami source. A linear combination of the pre-computed database is then performed based on this tsunami source, now reflecting the transfer of energy to the fluid body, to produce synthetic boundary conditions of water elevation and flow velocities to initiate the forecast model computation.

Accurate forecasting of the tsunami impact on a coastal community largely relies on the accuracies of bathymetry and topography and the numerical computation. The high spatial and temporal grid resolution necessary for modeling accuracy poses a challenge in the run-time requirement for real-time forecasts. Each forecast model consists of three telescoped grids with increasing spatial resolution in the finest grid, and temporal resolution for simulation of wave inundation onto dry land. The forecast model utilizes the most recent bathymetry and topography available to reproduce the correct wave dynamics during the inundation computation. Forecast models, including the Palm Beach, Florida model, are constructed for at-risk populous coastal communities in the Pacific and Atlantic Oceans. Previous and present development of forecast models in the Pacific (Titov *et al.*, 2005; Titov, 2009; Tang *et al.*, 2008; Wei *et al.*, 2008) have validated the accuracy and efficiency of each forecast model currently implemented in the real-time tsunami forecast system. Models are tested when the opportunity arises and are used for scientific research. Tang *et al.*, 2009 provide forecast methodology details.

### **3. Model Development**

The general methodology for modeling at-risk coastal communities is to develop a set of three nested grids, referred to as A, B, and C-grids, each of which becomes successively finer in resolution as they telescope into the population and economic center of the community of interest. The offshore area is covered by the largest and lowest resolution A-grid while the near-shore details are resolved within the finest scale C-grid to the point that tide gauge observations recorded during historical tsunamis are resolved within expected accuracy limits. The procedure is to begin development with large spatial extent merged bathymetric topographic grids at high resolution, and then optimize these grids by sub sampling to coarsen the resolution and reduce the overall grid dimensions to achieve a 4 hr simulation of modeled tsunami waves within the required time period of 10 min of wall-clock time. The basis for these grids is a high-resolution digital elevation model constructed by the National Geophysical Data Center and NCTR using all

available bathymetric, topographic, and shoreline data to reproduce the wave dynamics during the inundation computation for an at-risk community. For each community, data are compiled from a variety of sources to produce a digital elevation model referenced to Mean High Water in the vertical and to the World Geodetic System 1984 in the horizontal (<http://ngdc.noaa.gov/mgg/inundation/tsunami/inundation.html>). The author considers it to be an adequate representation of the local topography/bathymetry. As new digital elevation models become available, forecast models will be updated and report updates will be posted in [http://nctr.pmel.noaa.gov/forecast\\_reports/](http://nctr.pmel.noaa.gov/forecast_reports/). From these digital elevation models, a set of three high-resolution, “reference” elevation grids are constructed for development of a high-resolution reference model from which an ‘optimized’ model is constructed to run in an operationally specified period of time. The operationally developed model is referred to as the optimized tsunami forecast model or forecast model for brevity.

Development of an optimized tsunami forecast model for Palm Beach, Florida began with the spatial extent merged bathymetric/topographic grids shown in Figure 2. Grid dimension extension and additional information were updated as needed and appropriate. A significant portion of the modeled tsunami waves, 24 hrs of modeled tsunami time for Palm Beach, Florida, pass through the model domain without appreciable signal degradation. Table 1 provides specific details of both high resolution and tsunami forecast model grids, including extents and complete input parameter information for the model runs is provided in **Appendix A**.

### **3.1 Forecast area**

The town of Palm Beach, Florida is located on the east side of Palm Beach County and facing the Atlantic Ocean. It is a 16-mile barrier island with three bridges across the Intercoastal Waterway connecting it to the city of West Palm Beach (Figure 1) and is the second municipality that was incorporated into Palm Beach County on April 17, 1911. The location of the town of Palm Beach puts it closest to the Gulf Stream thus it has an outstanding marine environment, lush gardens and palm lined beaches (Government of Palm Beach). Although the population of the town is only 8,348 (U.S. Census Bureau 2010), it is the wealthiest community in the State of Florida and one of the most affluent in the entire United States (Delta Skyway Magazine, Dec 2010) with a median family income of US\$137,867 and per capita income of US\$109,219 (U.S. Census Bureau 2010).

The Intercoastal waterway is connected to the Atlantic Ocean thru several inlets. The widest inlet is located between the town of Palm Beach and Palm Beach Shores (Figure 1). There are lots islands inside the Intercoastal Waterway (Munyon Island, Little Munyon Island, Singer Island, Peanut Island, Everglades Island, Tarpon Island, Fisherman Island, Bingham Island, Hunters Island, Ibis Isle and Hypoluxo Island), also water inlets that goes further inland and the coast are lined with piers and docks. The deepest depth is about 13 meters and this is located in the Port of West Palm Beach where the tide gauge was previously installed (Figure 3). The shallowest is barely 1 meter in depth and these are usually inside the boat docking areas. At the entrance of the inlet, between Palm Beach Shores and Palm Beach, the depth is about 17 meters (Figure 3).

The highest elevation of the town of Palm Beach is close to 6 meters, where most of the highest elevation points are fronting the Atlantic Ocean, with a lowest at barely 1 meter.

As can be seen in Figure 3 the majority of the island barrier is just a few meters above water. A land elevation of barely 1 meter can easily be inundated by a large tsunami and the tsunami waves can quickly fill up the Intercoastal waterway and inundate the eastern side of Palm Beach County. For this reason, the forecast area also includes municipalities west of the Intercoastal Waterways. It covers the cities or town of Cloud Lake, Glen Ridge, Greenacres, Haverhill, Hypoluxo, Lake Clarke Shores, Lake Park, Lake Worth, Lantana, Manalapan, Mangonia Park, North Palm Beach, Palm Beach Gardens, Palm Beach Shores, Palm Springs, Riviera Beach, South Palm Beach and West Palm Beach (Figure 4). The total population of the included towns/cities is 315,666. The highest elevation of all the included municipalities is close to 13 meters however these are isolated in a small area and the general elevation is mostly below 6 meters (Figure 4).

### **3.2 Historical events and data**

In the Atlantic Basin, the Azores-Gibraltar plate boundary located in the Northern Basin is the source for the largest earthquake and tsunamis that could potentially affect the U.S. East Coast. The November 1, 1775 Lisbon earthquake was the largest tsunamigenic earthquake that occurred with an estimated magnitude ( $M_w$ ) of 8.5 – 9.0 (ten Brink, et al., 2008). Fortunately no tsunamigenic earthquake has occurred since then however, this would be difficult to validate the forecast model for Palm Beach, Florida. Although the historical tsunami source can still be used to simulate the generated tsunami waves and determine how it will affect Palm Beach, Florida.

Even if there were historical accounts of the 1775 Lisbon tsunami, tide gauge data would not be available since it was not established until May 1, 1967 in Palm Beach, Florida. The Port of West Palm Beach had a tide gauge installed on May 1, 1967 then removed on April 17, 1969. It was reinstalled on January 24, 2008 and removed again on October 20, 2010. It was located in the Intercoastal Waterway at  $80^\circ 3.1' W, 26^\circ 46.2' N$  (Figure 3). Currently the closest tide gauge station is in Lake Worth Pier with the coordinates  $80^\circ 2' W, 26^\circ 36.7' N$  which is out in the open ocean facing the Atlantic Basin (Figure 3). The closest point selected in the forecast model DEM as the tide gauge location is at  $80^\circ 1' 59.86'' W, 26^\circ 36' 42.33''$  with a depth of 4.74 meters. This was established on April 14, 1970 but the present installation was done on June 1, 2010. The tide gauge at Lake Worth Pier has a mean range of 2.73 feet (0.832 meters) and a diurnal range of 3.01 feet (0.918 meters). The station also shows that there is a mean sea level difference of 0.2 feet (0.06 meters) from a record range of 1960-1978 to 1983-2001 (Tides and Currents).

### **3.3 Model setup**

One unique feature of the U.S. East Coast is the existence of a very wide continental shelf. Also there are several islands (The Bahamas) located offshore of the town of Palm Beach (Figure 5). The existence of the continental shelf and several islands could potentially affect the simulated tsunami waves in the finest scale near-shore grid C if the domain size of the A-grid is not selected carefully. A total of 3 domain sizes were tested to determine if the extent of the A-grid would generate significant variation in the simulated tsunami waves. The DEM used for testing the domain extent of the A-grid has a 9 arc-sec grid resolution covering the U.S. East Coast and Gulf Coast and the Caribbean and was developed by NGDC (NGDC, 2005). The smallest A-grid is within the

continental shelf with the deepest depth of 825.5 meters. The largest A-grid extends beyond the continental shelf and well beyond into the deep ocean with a depth of 5400 meters. The medium size grid is just outside the continental shelf with a maximum depth of 5000 meters; see Table 2 and Figure 6. A synthetic scenario with an Mw= 9.5 was used to generate the tsunami waves propagating into the A-grid with the epicenter indicated in Figure 7.

The results of testing three different domain sizes for A-grid show a slight variation in the simulated tsunami wave height. Time series plots are compared at seven locations and also the maximum tsunami wave amplitude distribution. The locations where the tsunami time series are compared are indicated in Figure 8 while Figure 9a compares the time series and 9b compares the maximum tsunami wave amplitude. The three different grid A sizes indicate a very minimal variation in the tsunami waves and since the main objective of developing a forecast model is to provide a quick estimate of tsunami wave characteristics (i.e. wave arrival time, wave height, and inundation) minutes following a tsunami event, the smallest grid-A (with less computational nodes) will be used in the forecast model.

The high resolution Digital Elevation Model (DEM) for Palm Beach, Florida was developed by NGDC (Friday et al., 2010) with a grid resolution of 1/3 arc-seconds and coverage from 80.3600W to 79.4200W and 26.2900N to 27.3100 (Figure 2). The deepest water depth covered by the domain is 796.3 meters and the highest topography elevation is 26.37 meters. The DEM for the high resolution reference inundation model and the forecast model was extracted directly from the DEM developed by NGDC. Both high resolution reference inundation model and forecast model consists of three nested grid where the outer most grid (Grid A) covers the deep ocean region so as to capture the tsunami characteristics as it propagates in the deep ocean while the inner most grid (Grid C) covers the area outside the coral reef to capture the tsunami wave transformations in shallow waters.

The coverage extent of both high resolution reference inundation model and forecast model are the same. Table 1 shows the details of the nested grid (Grids A, B and C) including the modeling parameters used. The plots of the nested grids are shown in Figures 10 and 11 for the high resolution inundation model and forecast model, respectively. The forecast model, which is used for tsunami forecast during an event, is an optimized version of the high resolution inundation model. It is designed so that it can quickly provide 4 hours of simulated tsunami wave characteristics which includes time series at the tide gauge. For the town of Palm Beach, Florida, the forecast model can simulate the tsunami wave characteristics in approximately 9.7 minutes (Table 1). The high resolution inundation model on the other hand takes about 3.3 hours to complete a simulated run of 4 hours. Neither the high resolution inundation grid nor the forecast model was not validated with historical events to check for accuracy since there are no historical records/accounts available. However, simulation of the historical source was done to determine how the tsunami wave would affect the town of Palm Beach, Florida. The stability and reliability of both high resolution reference inundation grid and forecast model were tested by running synthetic scenarios with earthquake magnitudes (Mw) of 9.4, 7.5 and ~0 as listed in Table 3 with Figure 12 showing their locations.

## **4. Results and Discussion**

### **4.1 Model validation**

The development of the DEM for the high resolution reference inundation model and forecast model requires that it be validated to determine the accuracy of the simulated tsunami characteristics as it hits the coastal areas of Palm Beach, Florida. The largest tsunamigenic earthquake to occur in the Atlantic Basin was the 1775 Lisbon. Unfortunately there are no historical data since the earliest tide gauge was not established until May 1, 1967. Also there are no historical accounts of tsunami waves arriving at the coast of Palm Beach, Florida. However, the historical tsunami source (ten Brink et al, 2008) can still be used to determine how the generated tsunami wave would affect Palm Beach, Florida.

The other method to validate the forecast model is to compare the tsunami wave characteristics with the high resolution model. A higher resolution DEM should provide finer distributions of the tsunami wave pattern which might not be reflected in a forecast model due to a coarser resolution. This is a compromise since the forecast model is designed to provide a quick forecast a coarser resolution is need however, the deviation with the higher resolution model should not be too significant. Comparison between the forecast model and high resolution model will be evaluated by looking at the tide gauge time series and distribution of the maximum tsunami wave amplitude in grids A, B and C.

### **4.2 Model stability and reliability**

The development of the forecast model requires that the model provides a reliable forecast and should be stable enough to simulate several hours of the tsunami event. A set of reliability and stability tests was conducted by simulating synthetic events emanating from different regions and using different earthquake magnitudes ( $M_w = 9.3, 7.5$  and  $0$ ). Since each tsunami event is unique, tests using different earthquake magnitudes and source locations would indicate if the model grid developed will generate instabilities that need to be corrected. This set of tests is not exhaustive however, representative cases from select sources should be sufficient. A total of five artificial mega-tsunamis ( $M_w = 9.4$ ) were generated from twenty unit sources with a slip value of thirty meters for each unit source. One case of  $M_w = 7.5$  uses one unit source with a slip of one meter while one case of  $M_w = 0$  is to tests the model for a no wave condition. The unit sources are from the propagation database developed at NCTR (Gica et al., 2008). Tests were conducted for a total of 24 hours simulation. The list of sources used are indicated in Table 3 for the artificial mega-tsunamis,  $M_w = 7.5$  and  $M_w = 0$ . The location in reference to Palm Beach, Florida is show in Figure 12.

### 4.3 Results of tested events

The development of the forecast model and high resolution model requires that it be compared with historical events for validation. Unfortunately there are no historical records for Palm Beach, Florida even for the 1755 Lisbon tsunami which was documented in Europe. Validation will be done by comparing the simulated tsunami wave characteristics between the forecast model and high resolution model since it is expected that the higher resolution would provide a finer distribution of tsunami wave patterns. The tsunami time series at Lake Worth Pier tide gauge compares really well between the forecast model and high resolution model (Figure 13). The mega-events scenarios emanating from the Caribbean region had an almost perfect match for the entire time series. The mega-event scenario from South Sandwich Island has some slight variation in the later waves while the 1755 Lisbon had slight variation on the fourth to sixth wave (Figure 13, time series all sources). In terms of maximum tsunami wave amplitude distribution between the forecast model and the high resolution model, the distribution in grids A, B and C for all mega-events and 1755 Lisbon run are very similar (Figures 14-27) with the exception of the offshore of grid C for case atsz58-67 (Figures 20 and 21) . The distribution of the maximum tsunami wave amplitude for the forecast model outside the Intercoastal inlet is slightly lower as compared with the high resolution model (Figures 20 and 21). However, the variation is approximately less than 5 centimeters. Inside the Intercoastal waterway the maximum tsunami wave amplitude distribution is very similar for all scenarios (Figures 14-27, C grid). The obvious difference is at the inlet entrance between Palm Beach and Palm Beach Shores and around the area where the Port of West Palm Beach and Peanut Island (Figure 1) is located (Figures 14-27, C grid). This section has a deeper water depth for the ships to navigate into Port of West Palm Beach and with a relatively long narrow entrance into the Intercoastal waterway; a higher resolution grid is needed to describe the tsunami wave characteristics. It can be seen in Figures 14-27 (C grid) that the forecast model, using a coarser grid resolution of 2 arc-second, shows a slightly higher (less than 5 cm) distribution of maximum tsunami wave amplitude as compared with the higher resolution model which uses 2/3 arc-second.

The synthetic events ( $M_w=9.4$ , 7.5 and  $\sim 0$ ) simulated for the forecast model showed that it is both stable and reliable. Although the mega-tsunami ( $M_w = 9.4$ ) tests are not exhaustive, the results can indicate which tsunami source regions would pose a threat to Palm Beach, Florida. Plots of the maximum tsunami wave amplitude distribution are shown in Figures 14 - 27 while Figure 13 is the tsunami time series at the tide gauges for all scenarios simulated. Simulated results indicate that source scenarios (mega-events) atsz48-57 (Figures 18 and 19) and atsz58-67 (Figures 20 and 21) generated much higher tsunami waves offshore of Palm Beach, Florida (C grid) as compared to others. This is because the two mega-events (atsz48-57 and atsz58-67) are located on the northern end of the Caribbean and directly facing the open ocean (Figure 12). However, all the simulated mega-events show that Palm Beach, Florida is safe from seismically generated tsunamis emanating from the Caribbean and Europe (based on 1755 Lisbon tsunami). The incoming tsunami waves along the coast and into the intercoastal waterway barely generate any inundation. The tsunami energy generated from sources (Gica et al., 2008) in the Caribbean is trapped inside the Caribbean Sea with very minimal energy leaking out. Although there are quite a number of sources (Gica et al., 2008), along the northeast

and east side, that is facing the Atlantic Ocean, the existence of the large continental shelf and the Bahamas on the East blocks and quickly dissipates the tsunami energy. Similarly for the 1755 Lisbon tsunami where the continental shelf also minimizes the impact of the incoming tsunami waves into Palm Beach, Florida.

## **5. Summary and Conclusion**

A set of high resolution inundation model and forecast model has been prepared for Palm Beach, Florida. During the development instabilities occurred due to the existence of extreme shallow regions inside the intercoastal waterways. These locations were corrected manually or smoothing a cluster of nodes if the single node causing the instability is not located. Although there were corrections made to the DEM both models were found to be reliable and the comparison between the high resolution model and forecast model showed good comparison at the tide gauge station and the distribution of the maximum tsunami wave amplitude in all the grids (i.e. grids A, B and C).

The stability tests showed that the forecast model is stable for a 24 hour simulation for synthetic sources with different earthquake magnitudes ( $M_w = 9.4, 7.5, \text{ and } \sim 0$ ) from different source regions. A total of 6  $M_w = 9.4$ , 1  $M_w = 7.5$  and 1  $M_w = \sim 0$  were simulated. The mega-tsunami events not only check the stability of the forecast model, it can also provide information on which source region is Palm Beach, Florida more susceptible to tsunamis. From the limited test scenarios conducted, the existence of the continental shelf and islands in the Bahamas (east of Palm Beach, Florida) quickly dissipates the tsunami energy thus having minimal effects on Palm Beach, Florida. Although a few test scenarios (i.e. ATSZ 58-67AB and ATSZ 68-77AB) did indicate some minor inundation north of Singer Island (Figure 1 for location and Figures 20 and 22 for inundation) for the high resolution model, this should not be of much concern. In reality there is a water passage way north of Singer Island (Figure 28) whereby the grid resolution did not fully capture. The simulation of the 1755 Lisbon tsunami also indicated that (if it were to occur at present time) it does not pose a threat to Palm Beach, Florida.

Since the main objective of developing the Palm Beach, Florida forecast model is for tsunami forecast, the DEM has been optimized to simulate 4 hours of tsunami wave characteristics in approximately 9.7 minutes. As presented in this report, the Palm Beach, Florida forecast model should be able to provide a reliable forecast during an event and is stable for a 24 hours simulation.

## **6.0 Acknowledgments**

This publication is contribution XXX from NOAA/Pacific Marine Environmental Laboratory and funded by the Joint Institute for the Study of the Atmosphere and Ocean (JISAO) at the University of Washington under NOAA Cooperative Agreement No. NA17RJ1232, JISAO contribution XXX. The author would also like to thank Lt. Lindsey Wright, NOAA Corps (for retrieving historical tide gauge data and testing of the forecast model in SIFT as reported in Appendix C) and Sandra Bigley (for comments, edits and formatting of this report).

## 7.0 References

Delta Skyway magazine, Dec 2010 issues ([DeltaSkywayMag.delta.com](http://DeltaSkywayMag.delta.com)).

Friday, D.Z., Taylor, L.A., Eakins, B.W., Carignan, K.S., Caldwell, R.J., Grothe, P.R., and Lim, E.D. (2010): Digital Elevation Models of Palm Beach, Florida: Procedures, Data Sources and Analysis. NOAA Technical Memorandum NESDIS NGDC.

Gica, Edison, M.C. Spillane, V.V. Titov, C.D. Chamberlin and J.C. Newman (2008): Development of the forecast propagation database for NOAA's Short-term Inundation Forecast for Tsunamis (SIFT), NOAA Tech. Memo OAR PMEL139, NOAA/Pacific Marine Environmental Laboratory, Seattle, WA, 89pp.

Government of Palm Beach, Florida, <http://palmbeach.govoffice.com>.

National Geophysical Data Center (2005): East Coast and Gulf Coast and Caribbean Nine Second Tsunami Propagation Grids Compilation Report, 1 Dec 2005.

Palm Beach County, <http://www.pbhistoryonline.org>.

Synolakis, C.E., E.N. Bernard, V.V. Titov, U. Kânoğlu and F.I. González (2008): Validation and verification of tsunami numerical models. *Pure and Applied Geophysics* 165(11-12), 2197-2228.

Tang, L., V.V. Titov, and C.D. Chamberlin (2009): Development, testing, and applications of site-specific tsunami inundation models for real-time forecasting. *J. Geophys. Res.*, 6, doi: 10.1029/2009JC005476, in press.

Ten Brink, U., Twichell, D., Geist, E., Chaytor, J., Locat, J., Lee, H., Buczkowski, B., Barkan, R., Solow, A., Andrews, B., Parsons, T., Lynett, P., Lin, J., and Sansoucy, M. (2008): Evaluation of Tsunami Sources with the Potential to Impact the U.S. Atlantic and Gulf Coasts, An Updated Report to the Nuclear Regulatory Commission, by the Atlantic and Gulf of Mexico Tsunami Hazard Assessment Group, revised August 22, 2008.

Tides and Currents, [www.tidesandcurrents.noaa.gov](http://www.tidesandcurrents.noaa.gov)

Titov, V.V. and F.I. Gonzalez (1997): Implementation and testing of Method of Splitting Tsunami (MOST) model. NOAA Tech. Memo. ERL PMEL-112 (PB98-122773), NOAA/Pacific Marine Environmental Laboratory, Seattle, WA, 11pp.

Titov, V.V., F.I. Gonzalez, E.N. Bernard, M.C. Eble, H.O. Mofjeld, J.C. Newman and A.J. Venturato (2005): Real-time tsunami forecasting: Challenges and solutions. *Natural Hazards*, 35, 41-58.

Titov, V.V. (2009): Tsunami forecasting. In *The Sea*, Vol. 15, Chapter 12, Harvard University Press, Cambridge, MA, and London, England, 371–400.

U.S. Census Bureau 2010, [factfinder2.census.gov](http://factfinder2.census.gov).

Wei, Y., E. Bernard, L. Tang, R. Weiss, V. Titov, C. Moore, M. Spillane, M. Hopkins, and U. Kânoglu (2008): Real-time experimental forecast of the Peruvian tsunami of August 2007 for U.S. coastlines. *Geophys. Res. Lett.*, 35, L04609, doi: 10.1029/2007GL032250.

Table 1. MOST setup parameters for reference and forecast models for Palm Beach, Florida.

		Reference Model				Forecast Model			
Grid	Region	Coverage	Cell	nx	Time	Coverage	Cell	nx	Time
		Lat. [°N] Lon. [°W]	Size [“]	x ny	Step [sec]	Lat. [°N] Lon. [°W]	Size [“]	x ny	Step [sec]
A	Palm	27.5000-25.8000	9	601 x 681	2.0	27.5000-25.8000	18	301 x 341	4.0
	Beach, FL	279.0000-280.5000				279.0000-280.5000			
B	Palm	27.0000-26.4000	6	241 x 361	2.0	27.0000-26.4000	9	161 x 241	4.0
	Beach, FL	279.7500-280.1500				279.7500-280.1500			
C	Palm	26.8482-26.5666	2/3	901 x 1522	0.4	26.8482-26.5666	2	301 x 508	1.0
	Beach, FL	279.8332-279.9999				279.8332-279.9999			
Minimum offshore depth [m]				1.0	1.0				
Water depth for dry land [m]				0.1	0.1				
Friction coefficient [n <sup>2</sup> ]				0.0009	0.0009				
CPU time for 4-hr simulation				3.3 hours	9.7 minutes				

Computations were performed on a Dell PowerEdge R510 with 2xHex-core Intel Xeon E5670 CPU processor at 2.93 GHz with 12M cache each.

Table 2. Grid extents used to determine the final A-grid size in the development of a forecast model and high resolution model.

Test A-Grid	Coverage	Cell	nx	Maximum
	Lat. [°N]	Size	x	Offshore Depth
	Lon. [°W]	[“]	ny	[meters]
Large	27.5000-25.8000	9	3201 x 681	5,400.0
	279.0000-287.0000			
Medium	27.5000-25.8000	9	2201 x 681	5,000.0
	279.0000-284.5000			
Small	27.500-25.8000	9	601 x 681	825.5
	279.0000-280.5000			

Table 3. Synthetic tsunamis tested for Palm Beach, Florida.

Scenario Name	Subduction Zone	Tsunami Source	Mw
ATSZAB 38-47	Atlantic	30 x (A38-47, B38-47)	9.4
ATSZAB 48-57	Atlantic	30 x (A48-57, B48-57)	9.4
ATSZAB 58-67	Atlantic	30 x (A58-67, B58-67)	9.4
ATSZAB 68-77	Atlantic	30 x (A68-77, B68-77)	9.4
ATSZAB 82-91	Atlantic	30 x (A82-91, B82-91)	9.4
SSSZAB 01-10	South Sandwich	30 x (A01-10, B01-10)	9.4
ATSZB52	Atlantic	1 x B52	7.5
SSSZB11	South Sandwich	0 x B11	~0.0

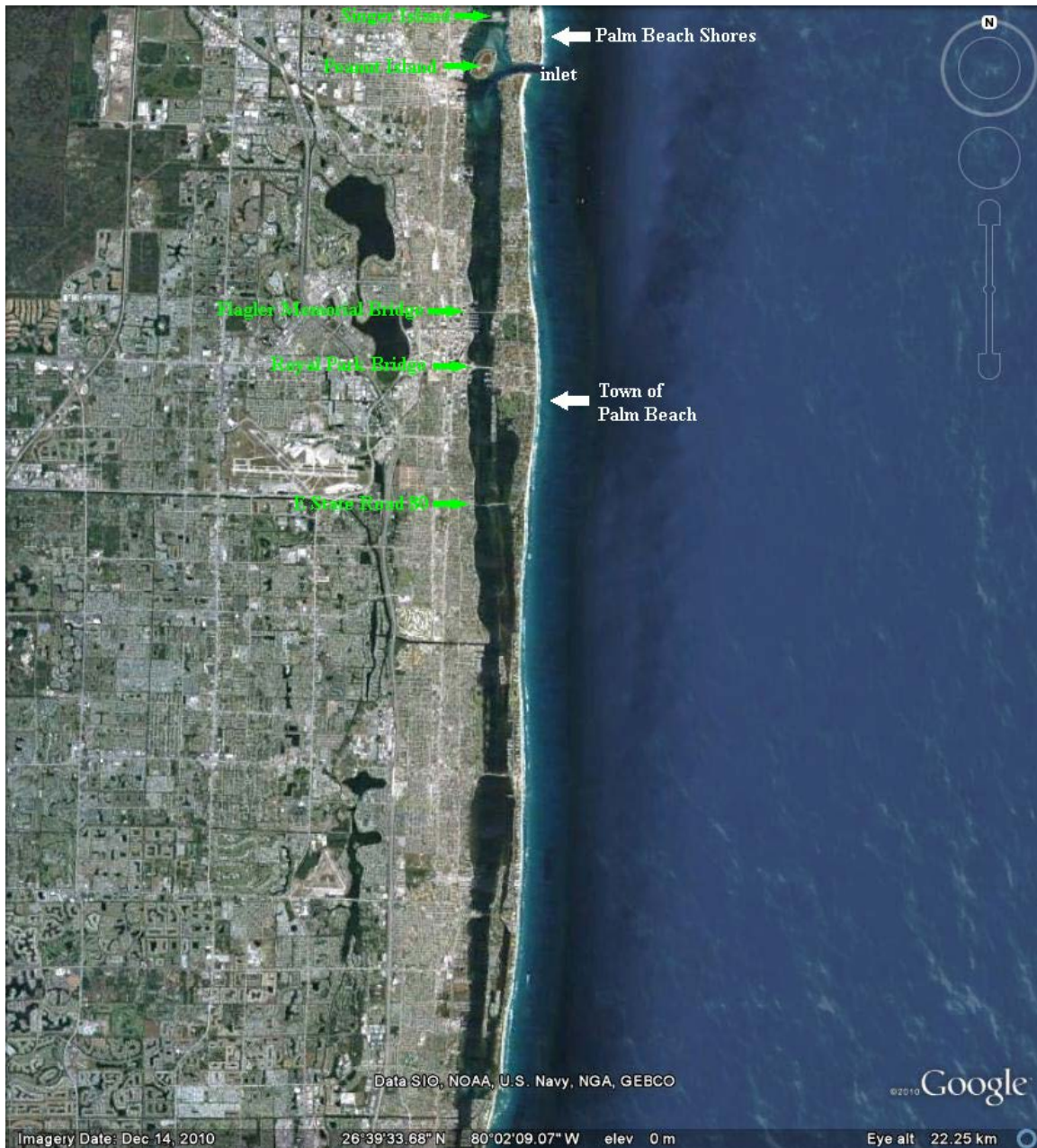


Figure 1. Google map image of Palm Beach, Florida with location of the inlet into the Intercoastal waterways and the three bridges (Flagler Memorial Bridge, Royal Park Bridge and E State Road 80) that connects the town to West Palm Beach on the western side.

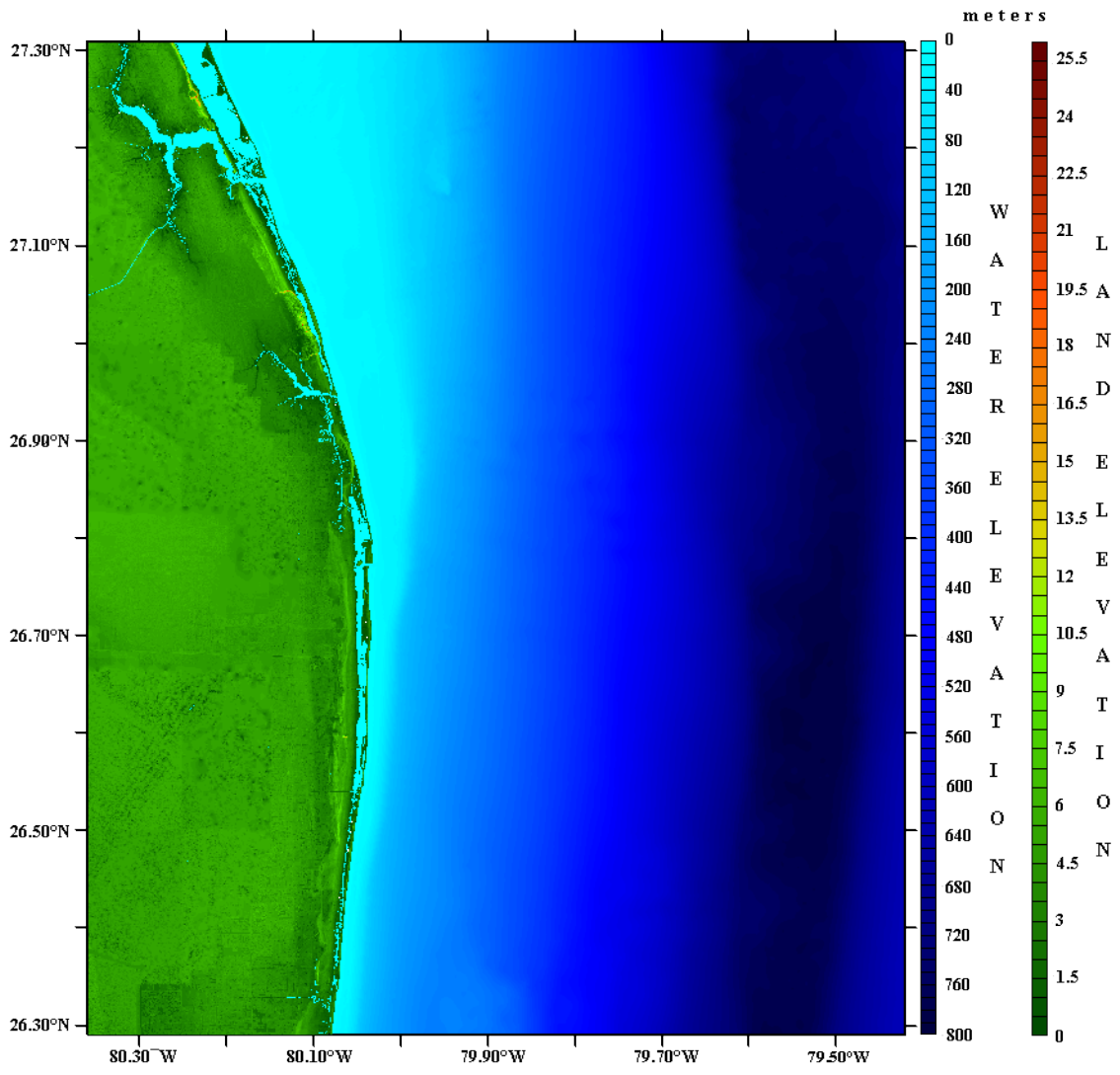


Figure 2. Plot of 1/3 arc-sec DEM developed by NGDC and used in the development of the forecast model.

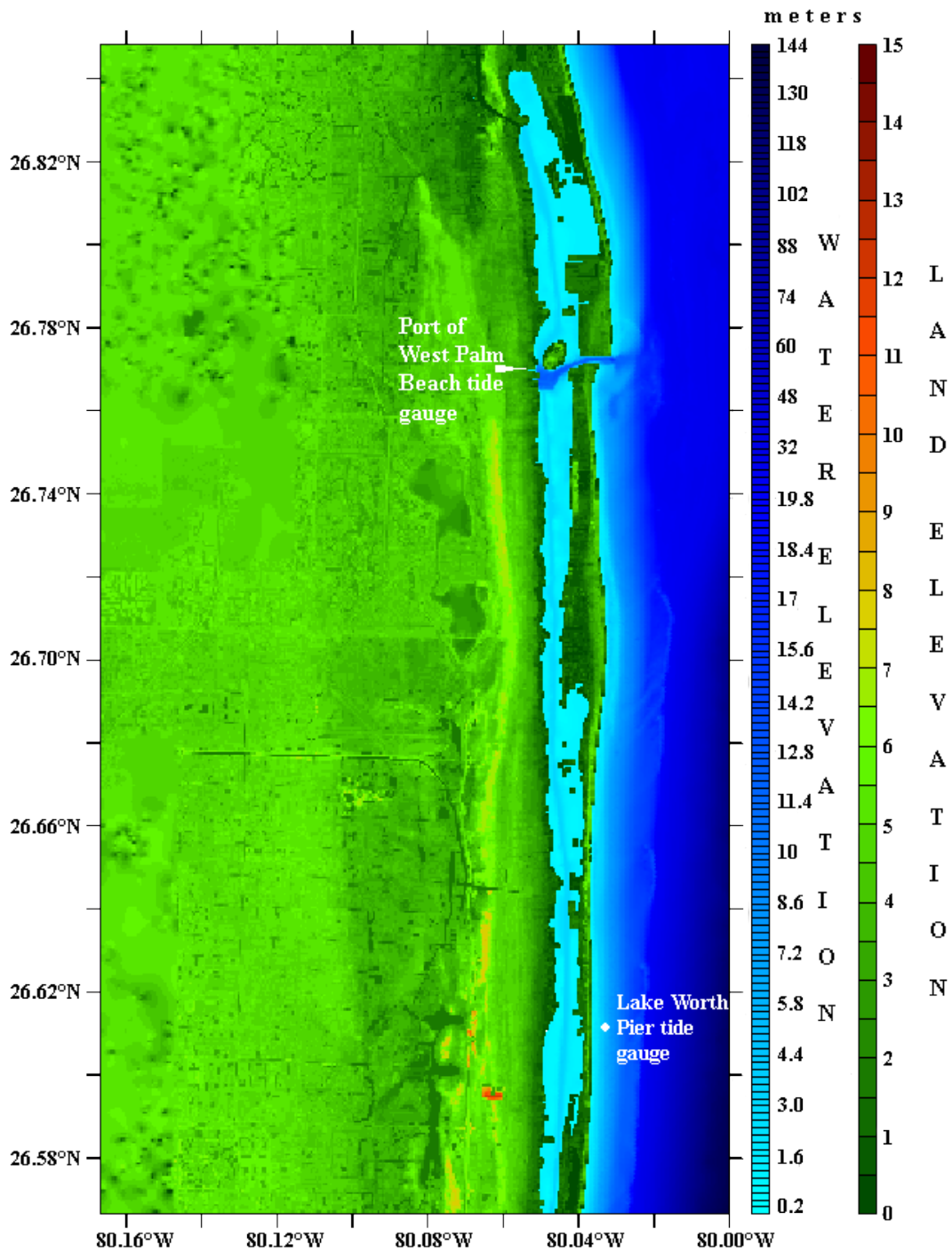


Figure 3. Plot of C-grid extent used in the development of the forecast model. The plot is based on a 1/3 arc-sec DEM developed by NGDC and also indicates the location of tide gauges in the region (Lake Worth Pier and Port of West Palm Beach). The tide gauge at Port of West Palm Beach was removed on October 20, 2010 (Tides and Currents).

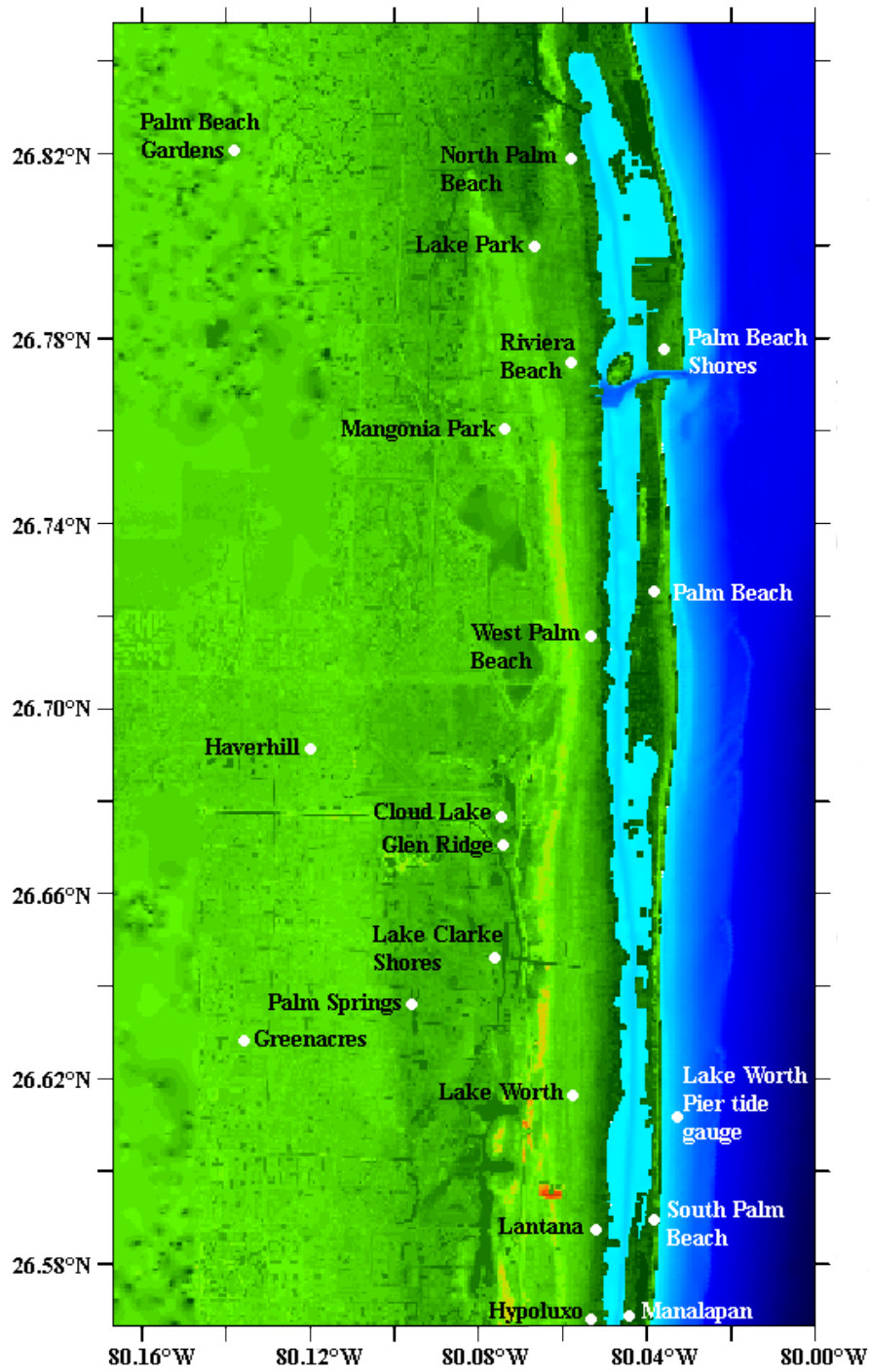


Figure 4. Plot of C-grid extent used in the development of the forecast model indicating cities and towns that are included.



Figure 5. Google map image showing the existence of the wide continental shelf and islands in the Bahamas relative to the location of Palm Beach, Florida.

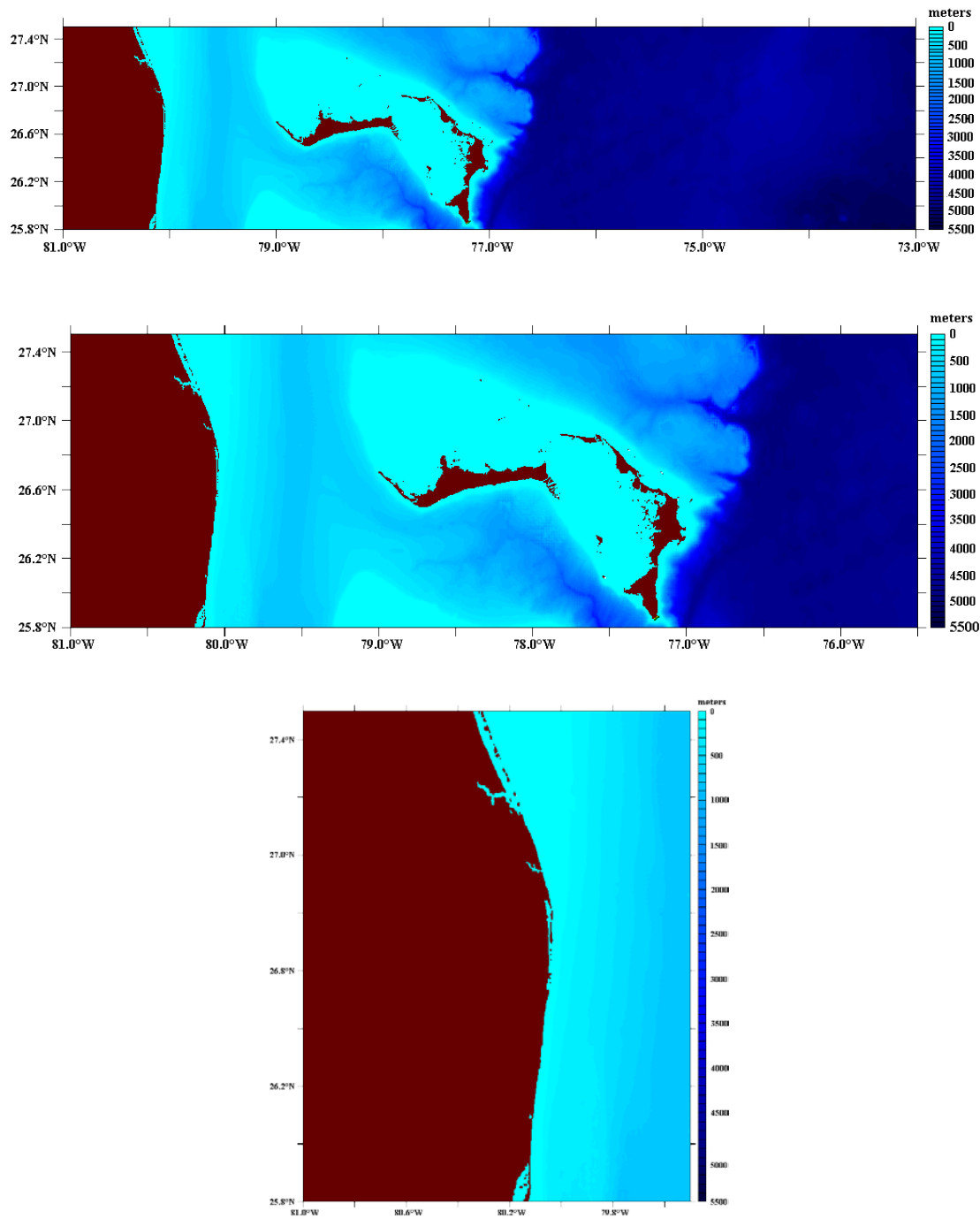


Figure 6. Plots of grid extent used to determine the final A-grid size in the development of a forecast model and high resolution model; top) Largest grid the covers a significant portion of the deep ocean, middle) medium size grid that still covers deep ocean, bottom) smallest grid the is on the continental shelf.

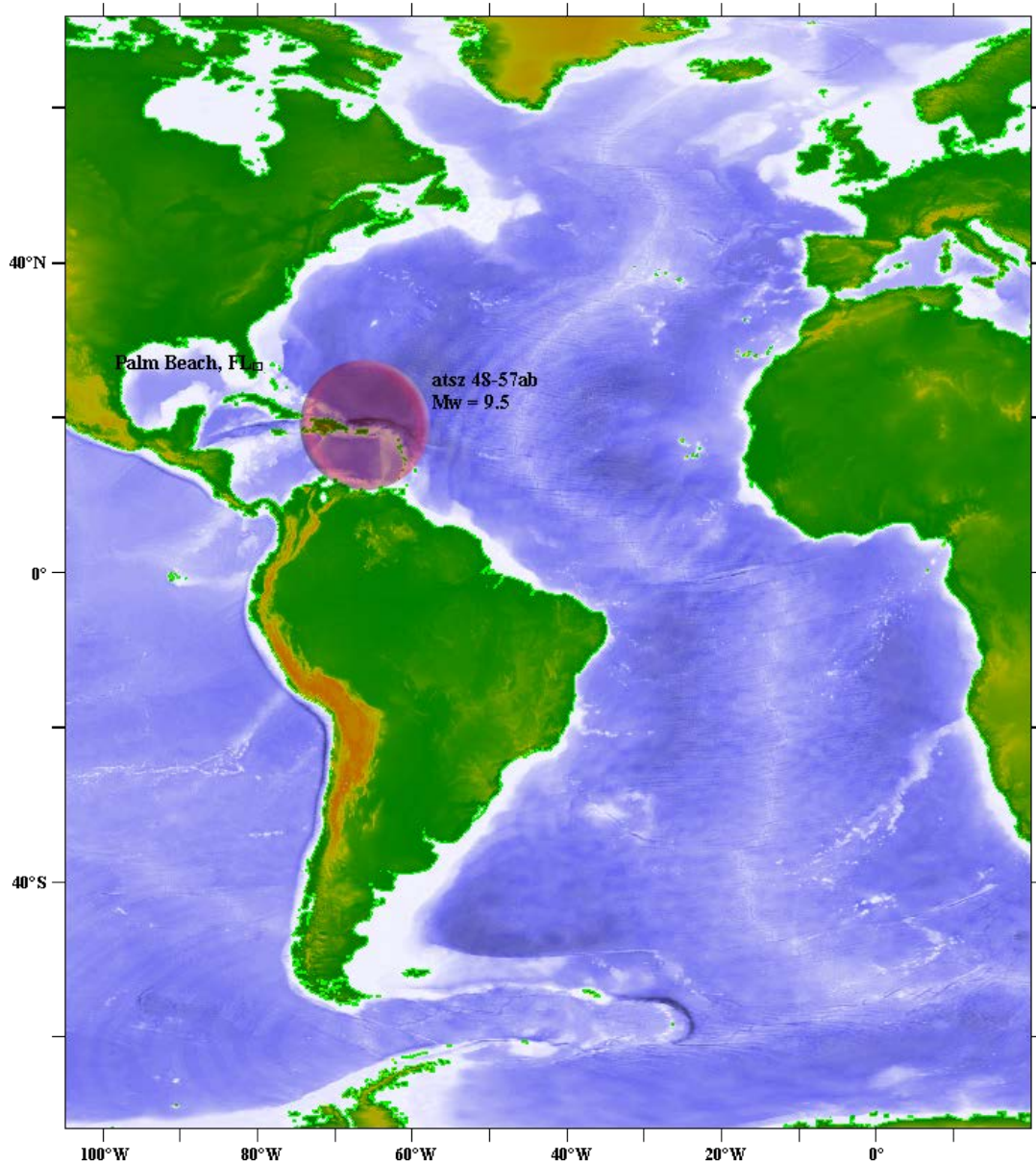


Figure 7. Location of a synthetic scenario ( $M_w=9.5$ ), relative to Palm Beach, Florida, used to test the domain size.

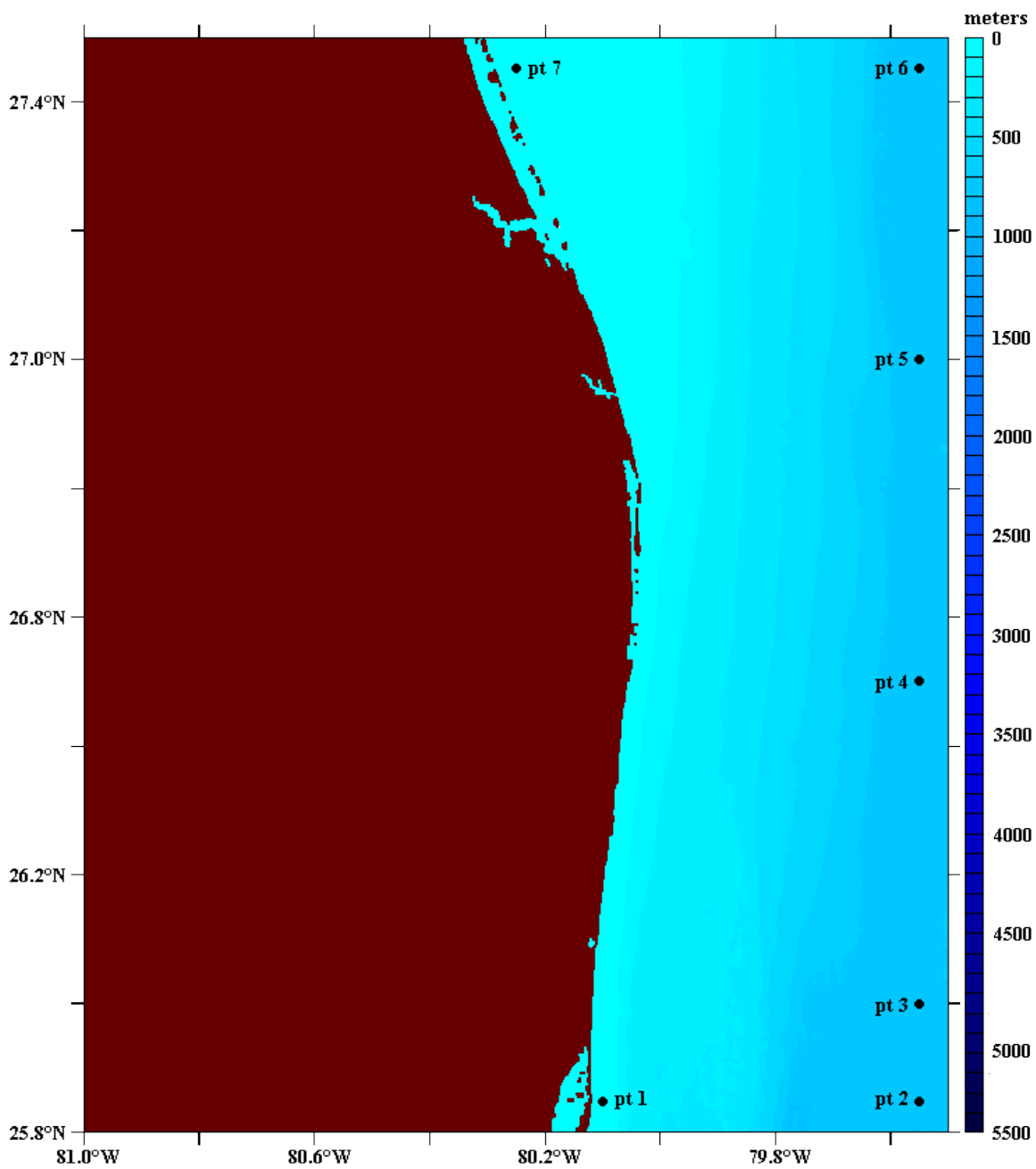


Figure 8. Location of points where time series are compared for testing different domain sizes (see Figure 7).

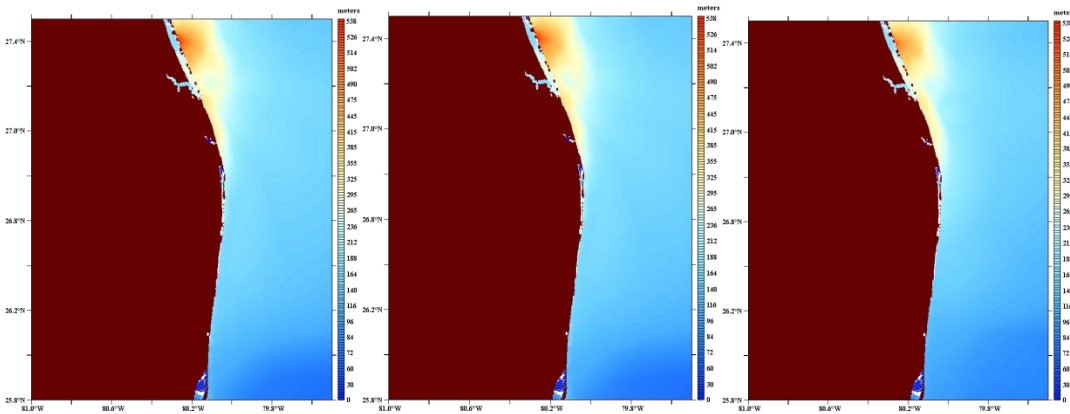
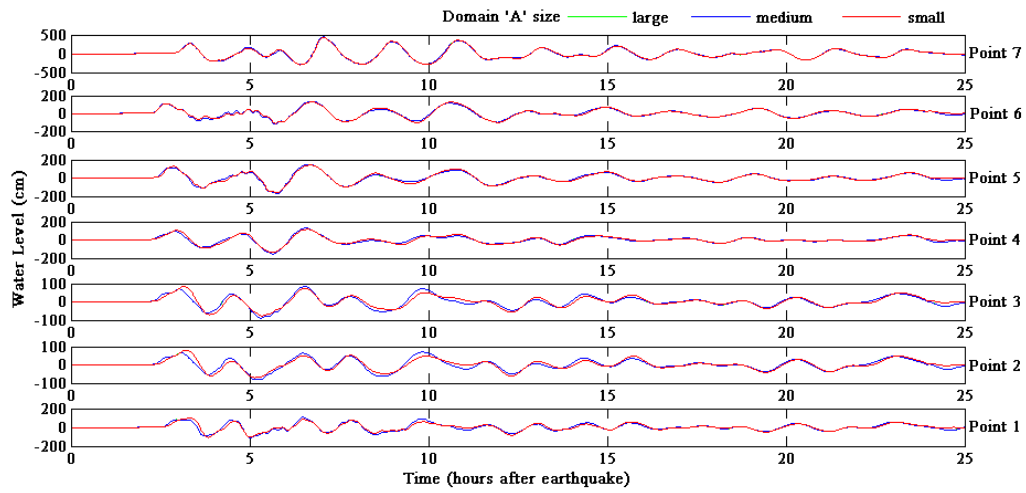


Figure 9. Comparison of time series plots (top) and maximum tsunami wave amplitude distribution (bottom-left-large domain, bottom-middle-medium domain and bottom-right small domain). The bottom plots of large domain (bottom-left) and medium domain (bottom-middle) are adjusted to match that of the small domain (bottom-right) for consistency.

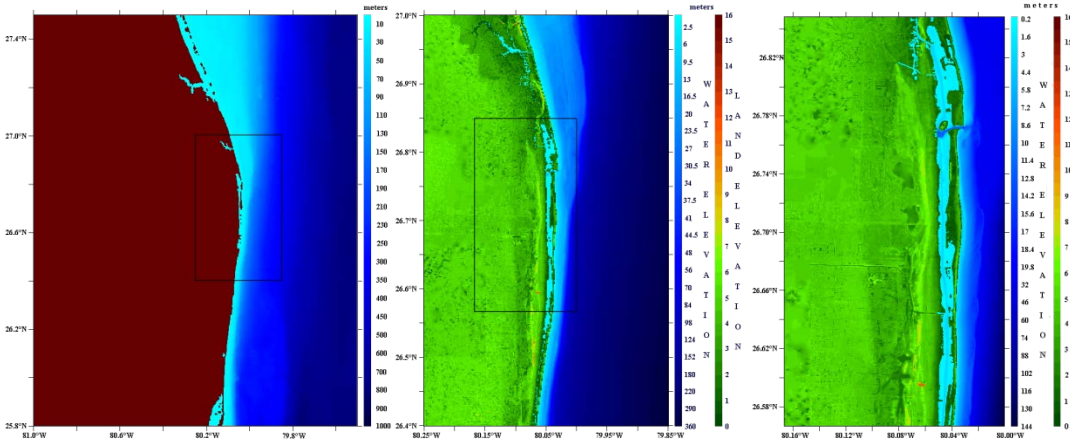


Figure 10. Plot of DEM used for the high resolution model; left) A- grid using a grid resolution of 9 arc-sec with the box indicating the location of B-grid, middle) B-grid using a grid resolution of 6 arc-sec with the box indicating the location of C-grid; right) C-grid using a grid resolution of 2/3 arc-seconds.

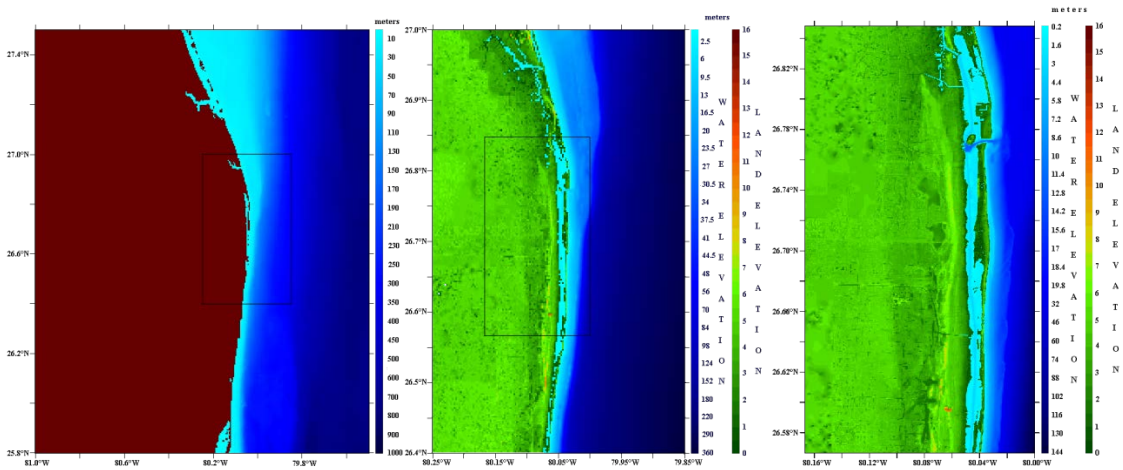


Figure 11. Plot of DEM used for the high resolution model; left) A- grid using a grid resolution of 18 arc-sec with the box indicating the location of B-grid, middle) B-grid using a grid resolution of 9 arc-sec with the box indicating the location of C-grid; right) C-grid using a grid resolution of 2 arc-seconds.

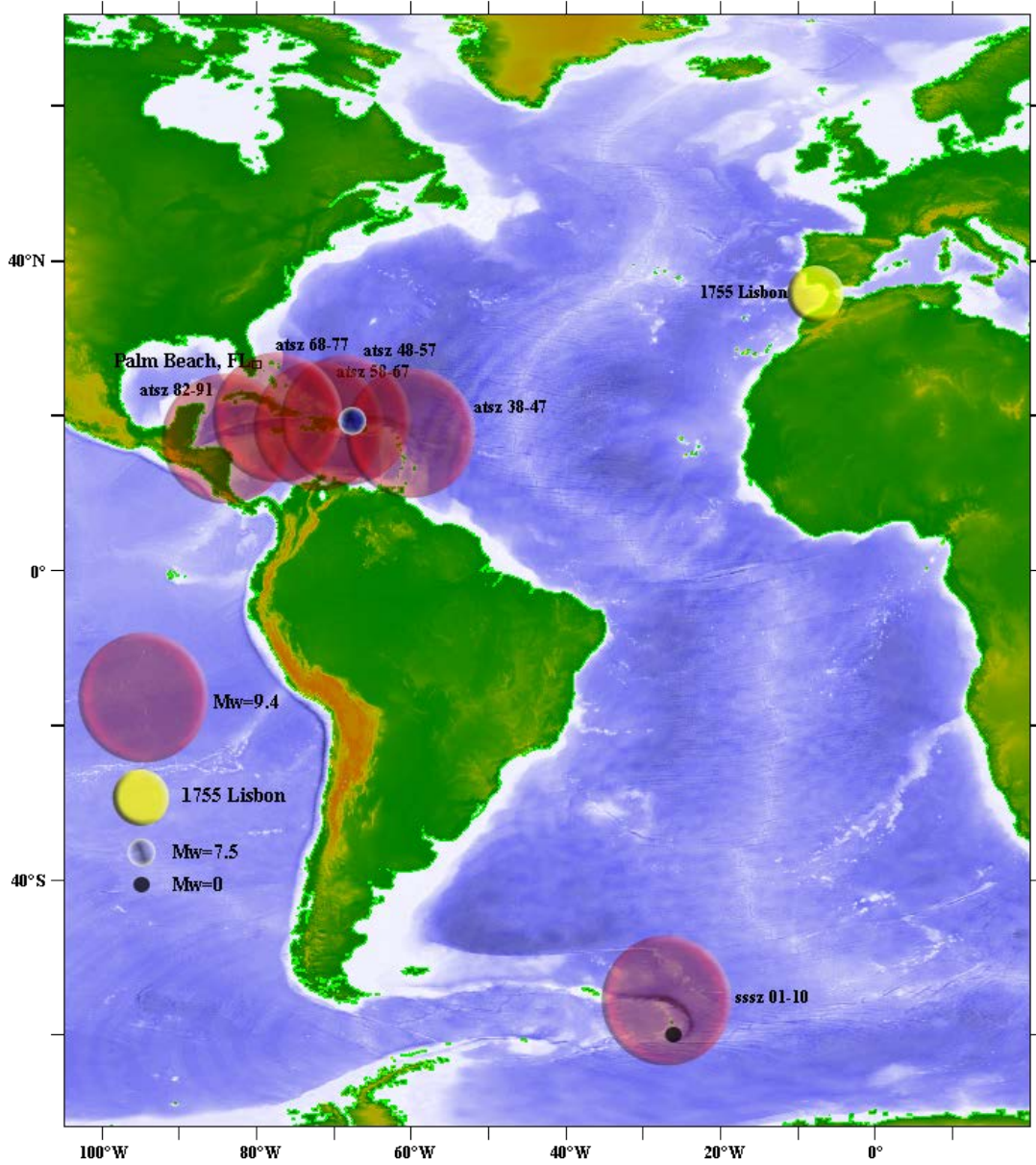


Figure 12. Plot locating the scenarios ( $M_w=9.4$ ,  $M_w=7.5$ ,  $M_w=\sim 0$  and 1755 Lisbon) used for testing the stability and reliability of the forecast model and high resolution model in relation to the location of Palm Beach, Florida.

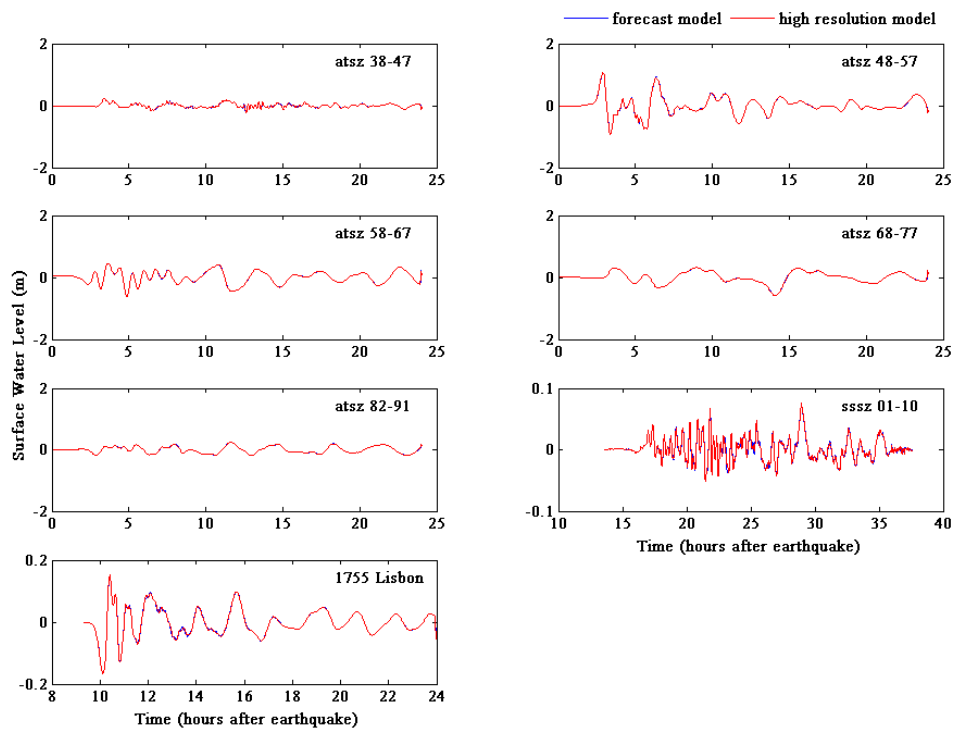


Figure 13. Time series comparison at Lake Worth Pier tide gauge between the forecast model and high resolution model for 1755 Lisbon and synthetic mega-events with  $M_w=9.4$ . Plot shows an almost perfect comparison with very slight variation for sssz01-10 and 1755 Lisbon.

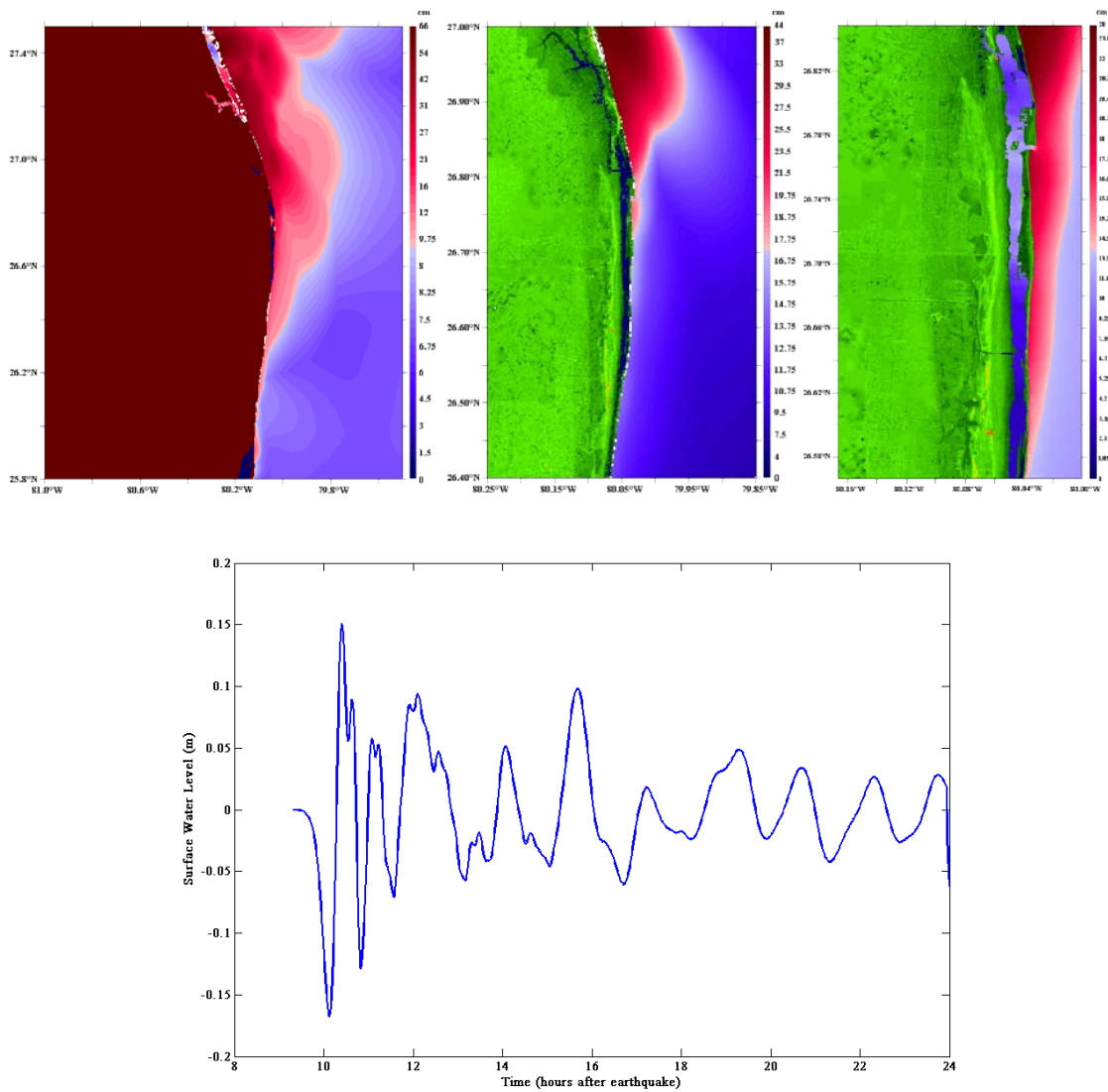


Figure 14. Plot of maximum tsunami wave amplitude distribution [left), A-grid; middle) B-grid and right) C-grid] and time series [bottom) at Lake Worth Pier tide gauge] for the 1755 Lisbon tsunami using high resolution model.

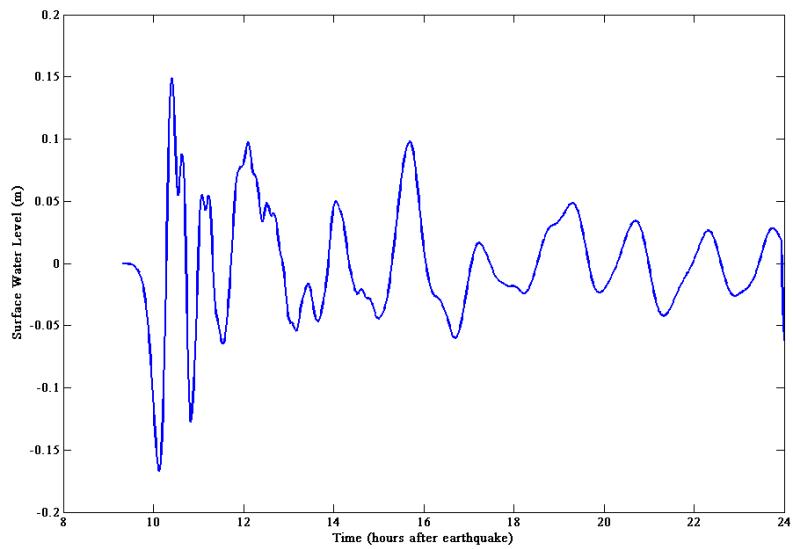
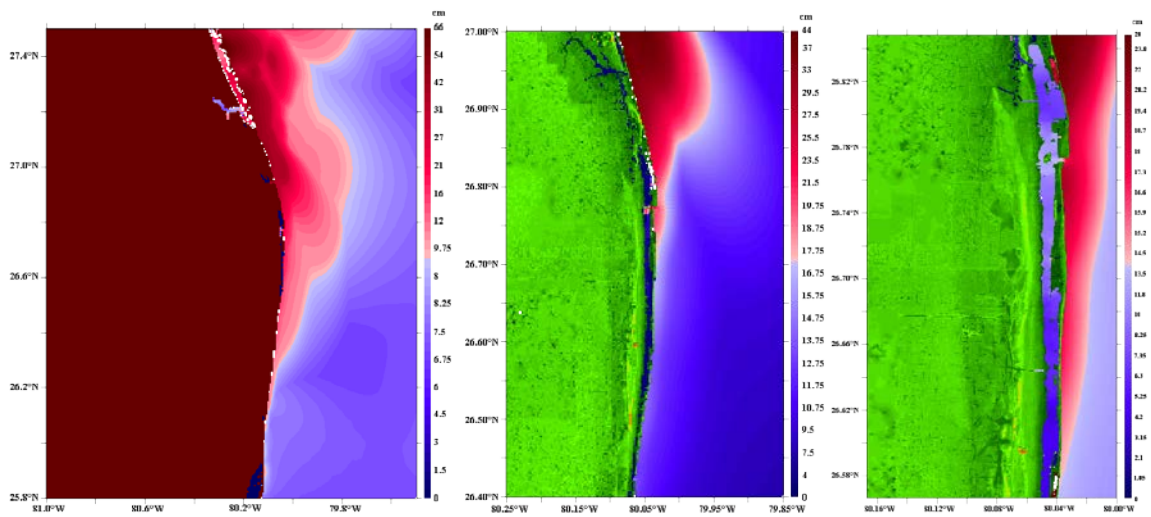


Figure 15. Plot of maximum tsunami wave amplitude distribution [left), A-grid; middle) B-grid and right) C-grid] and time series [bottom) at Lake Worth Pier tide gauge] for the 1755 Lisbon tsunami using forecast model.

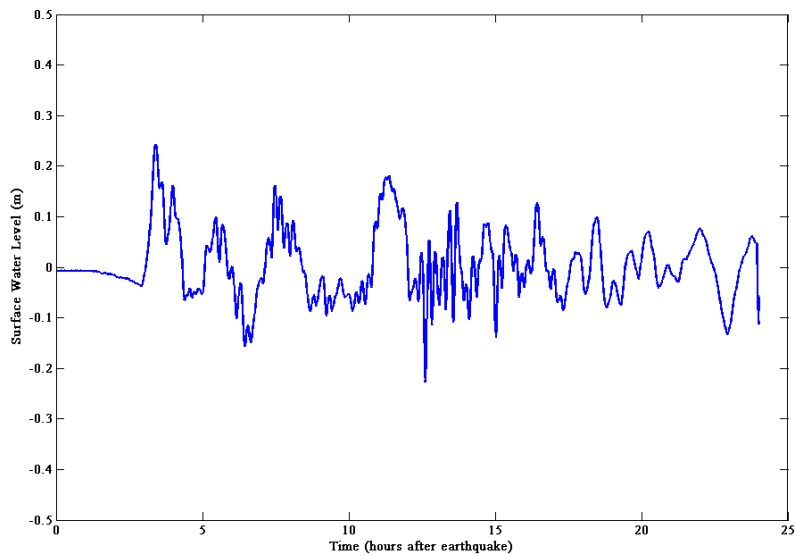
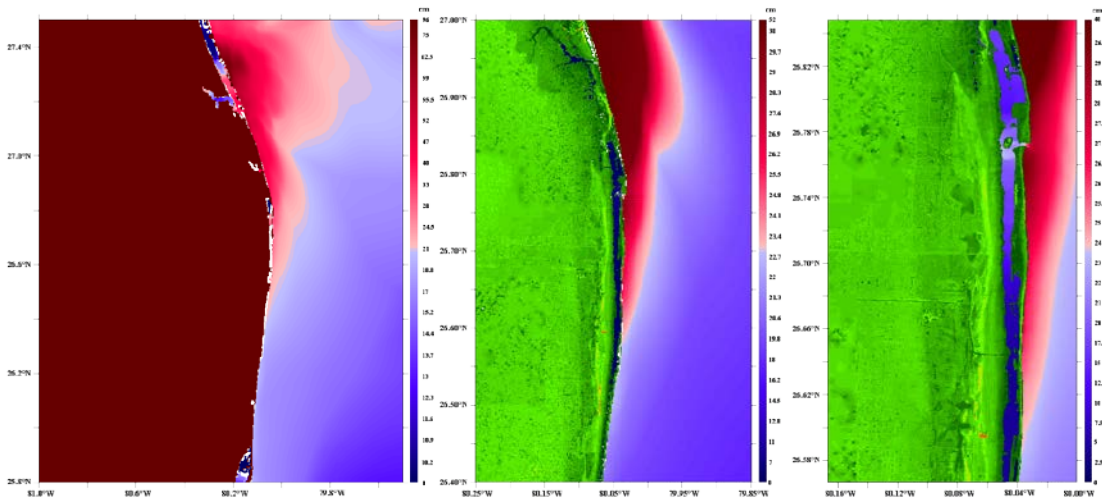


Figure 16. Plot of maximum tsunami wave amplitude distribution [left), A-grid; middle) B-grid and right) C-grid] and time series [bottom) at Lake Worth Pier tide gauge] for mega-event (Mw=9.4) case ATSZ38-47AB using high resolution model.

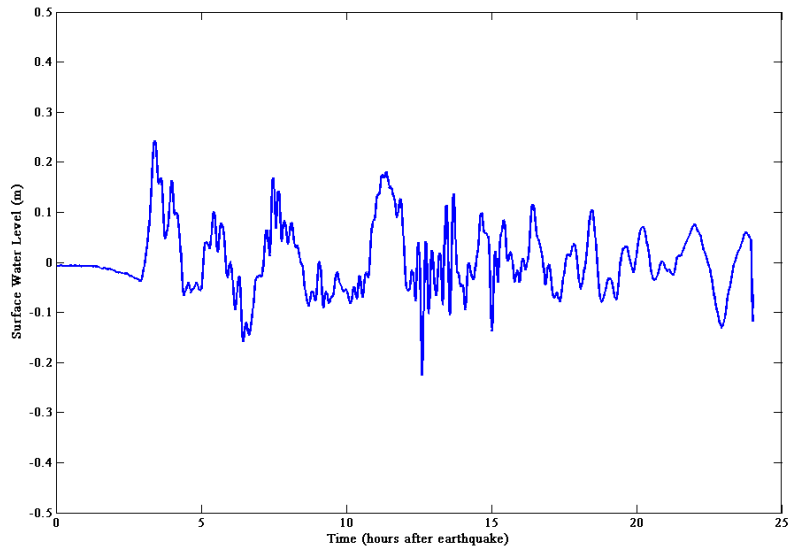
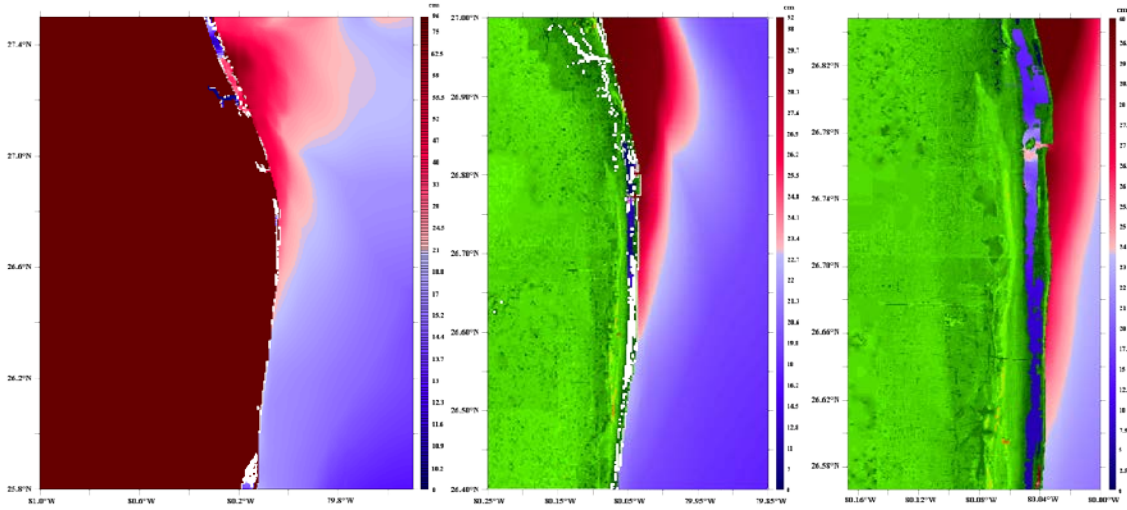


Figure 17. Plot of maximum tsunami wave amplitude distribution [a), A-grid; b) B-grid and c) C-grid] and time series [d) at Lake Worth Pier tide gauge] for mega-event (Mw=9.4) case ATSZ38-47AB using forecast model.

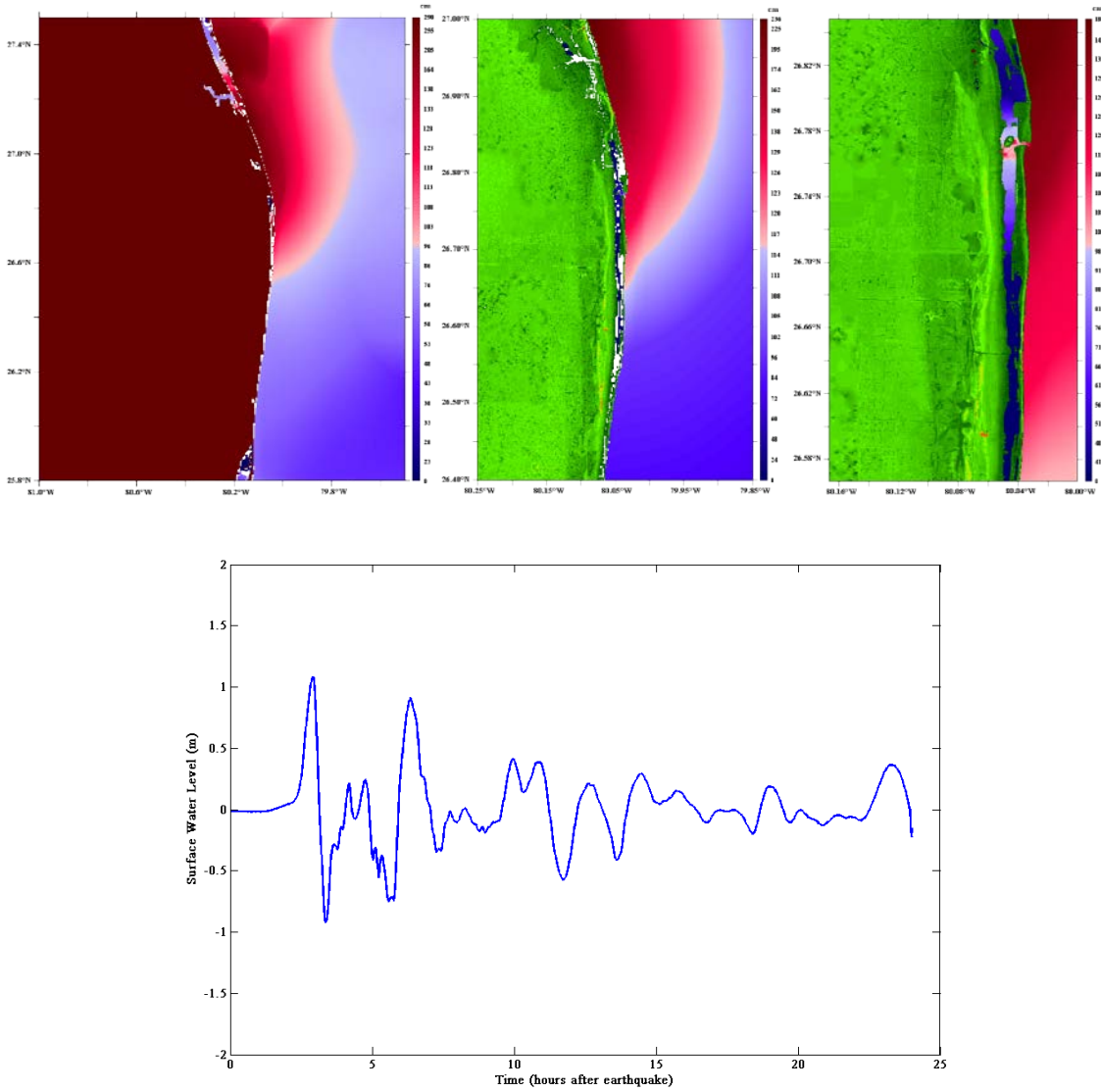


Figure 18. Plot of maximum tsunami wave amplitude distribution [left), A-grid; middle) B-grid and right) C-grid] and time series [bottom) at Lake Worth Pier tide gauge] for mega-event (Mw=9.4) case ATSZ48-57AB using high resolution model.

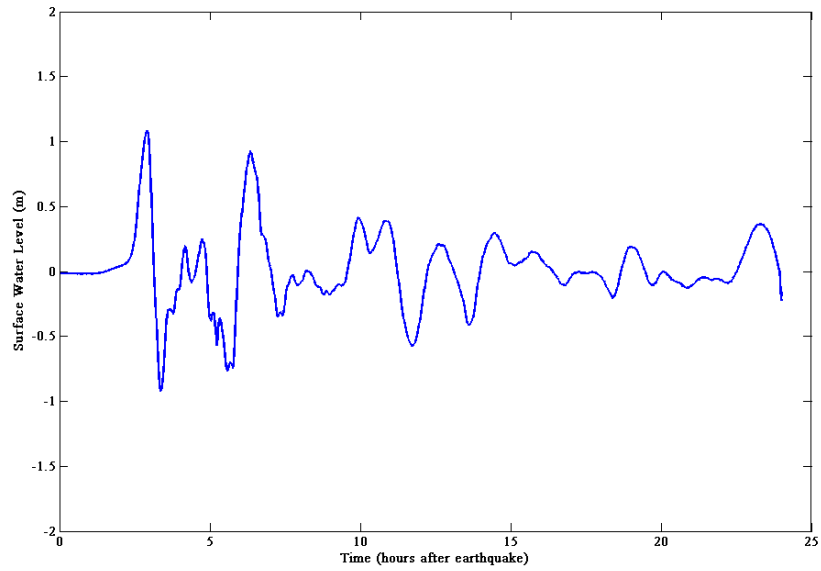
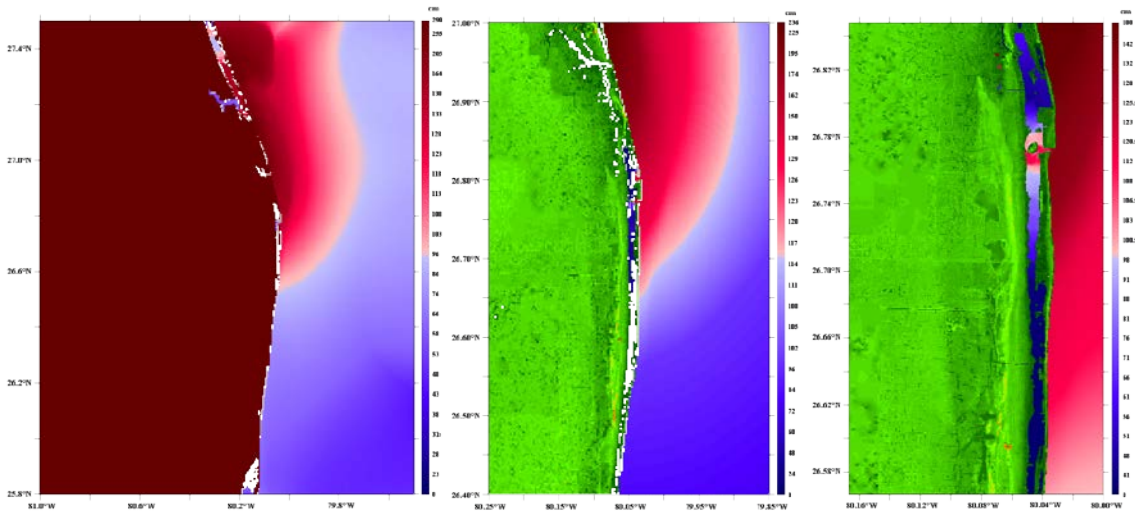


Figure 19. Plot of maximum tsunami wave amplitude distribution [left, A-grid; middle) B-grid and right) C-grid] and time series [bottom) at Lake Worth Pier tide gauge] for mega-event (Mw=9.4) case ATSZ48-57AB using forecast model.

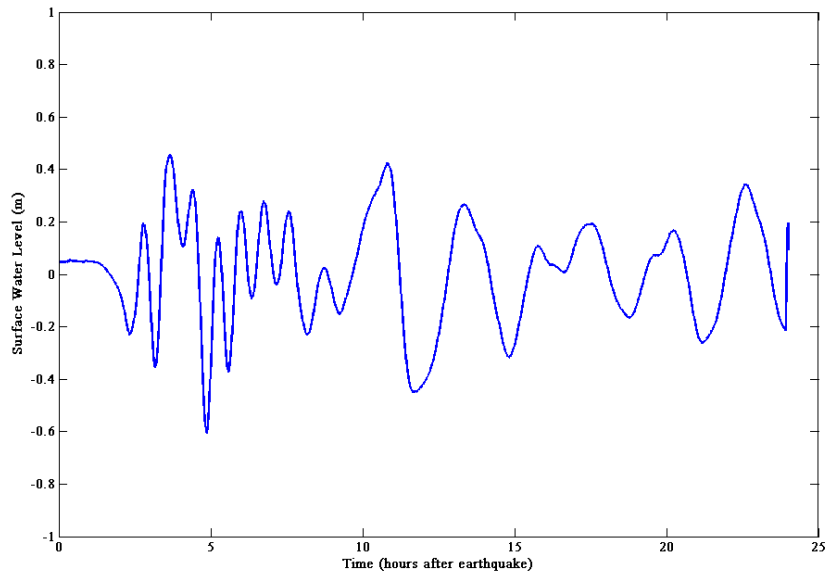
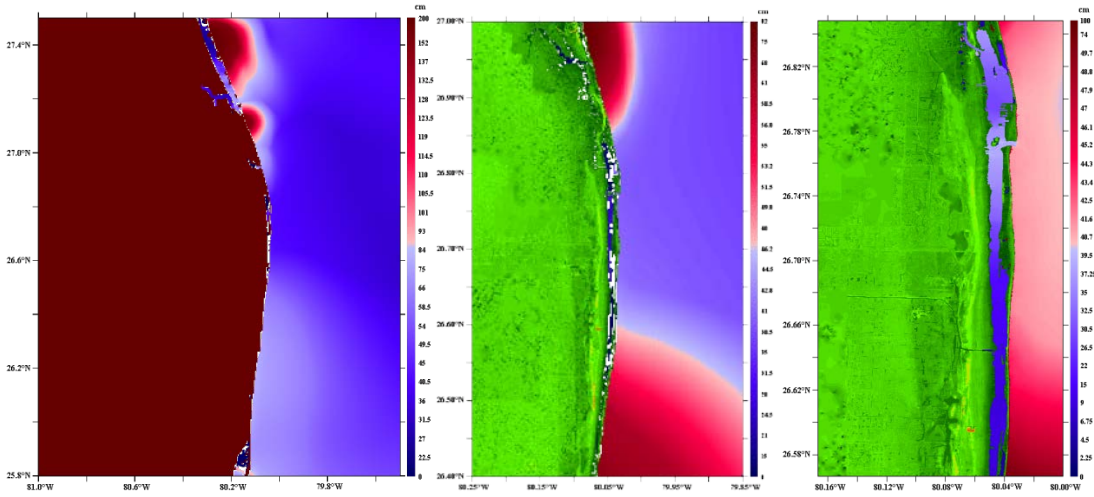


Figure 20. Plot of maximum tsunami wave amplitude distribution [left), A-grid; middle) B-grid and right) C-grid] and time series [bottom) at Lake Worth Pier tide gauge] for mega-event (Mw=9.4) case ATSZ58-67AB using high resolution model.

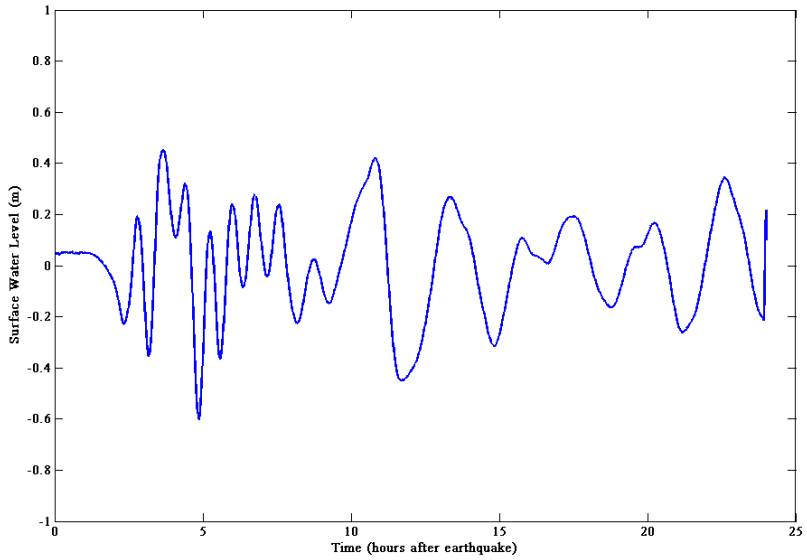
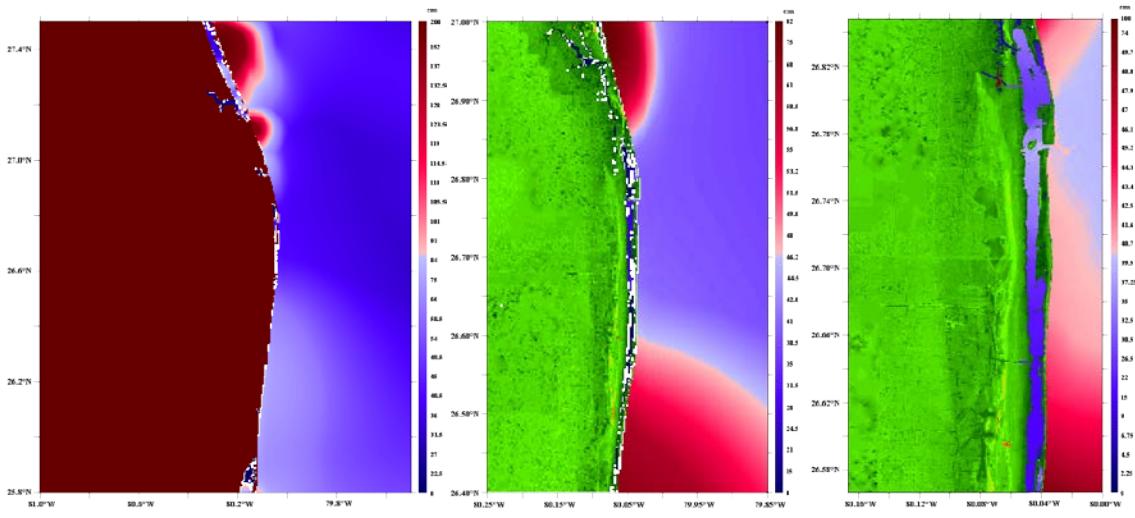


Figure 21. Plot of maximum tsunami wave amplitude distribution [left), A-grid; middle) B-grid and right) C-grid] and time series [bottom) at Lake Worth Pier tide gauge] for mega-event (Mw=9.4) case ATSZ58-67AB using forecast model.

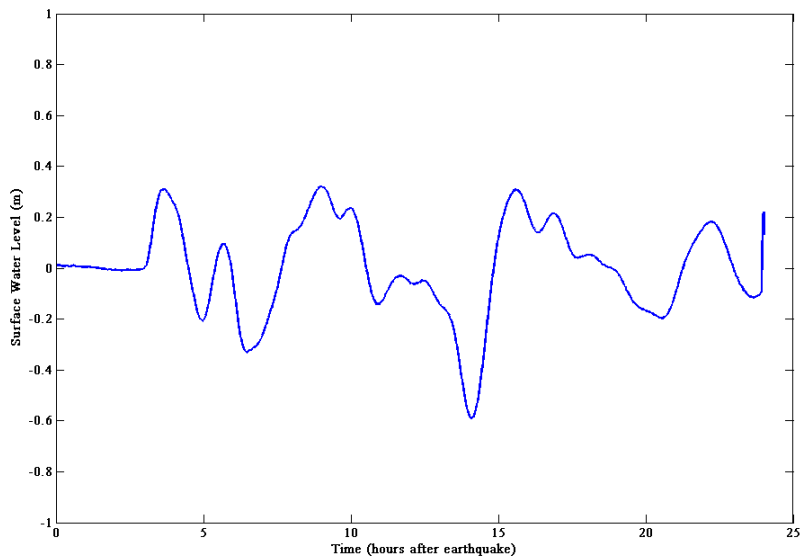
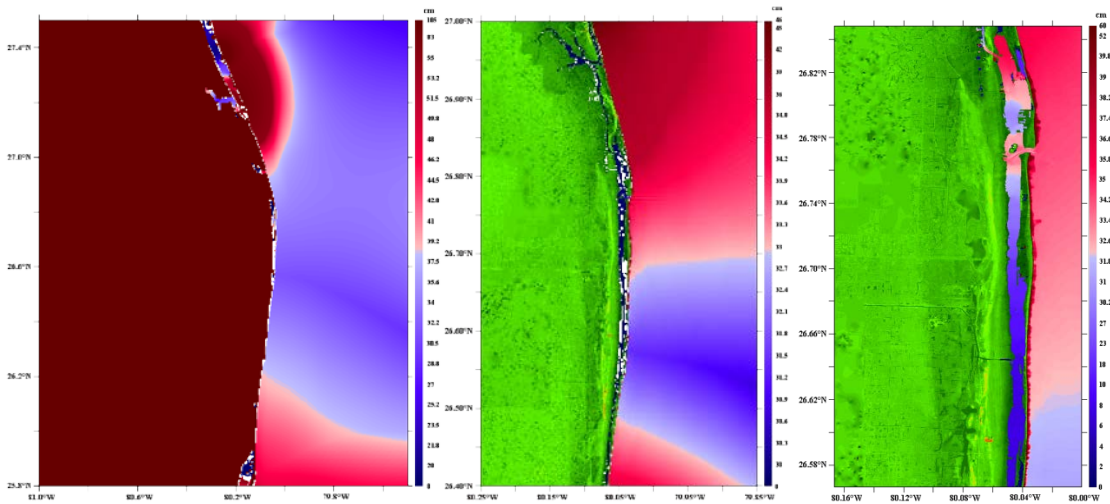


Figure 22. Plot of maximum tsunami wave amplitude distribution [left), A-grid; middle) B-grid and right) C-grid] and time series [bottom) at Lake Worth Pier tide gauge] for mega-event (Mw=9.4) case ATSZ68-77AB using high resolution model.

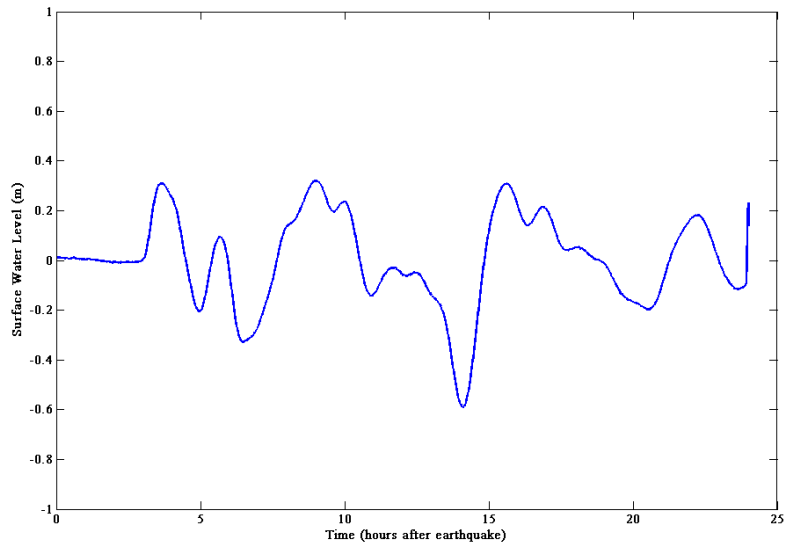
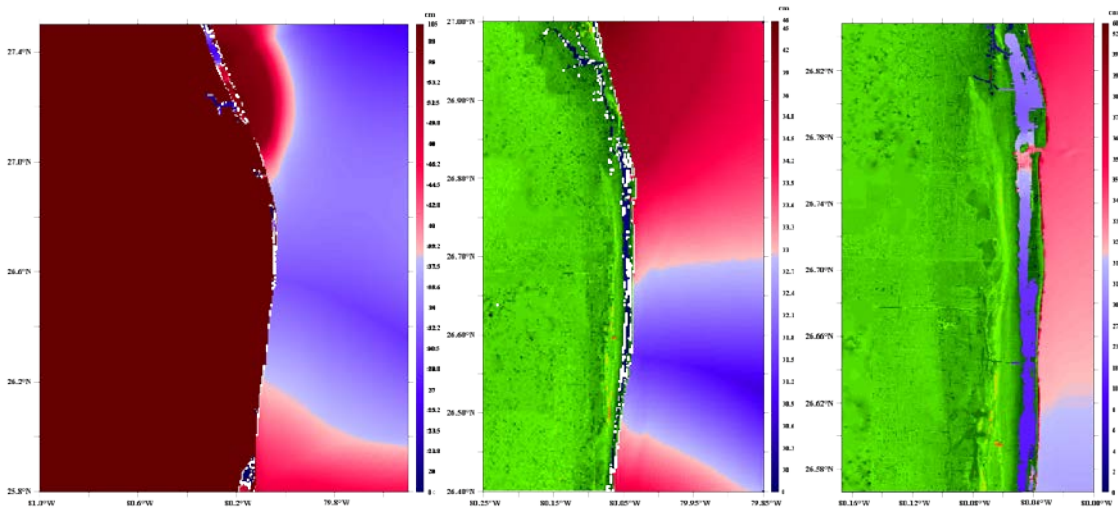


Figure 23. Plot of maximum tsunami wave amplitude distribution [left), A-grid; middle) B-grid and right) C-grid] and time series [bottom) at Lake Worth Pier tide gauge] for mega-event (Mw=9.4) case ATSZ68-77AB using forecast model.

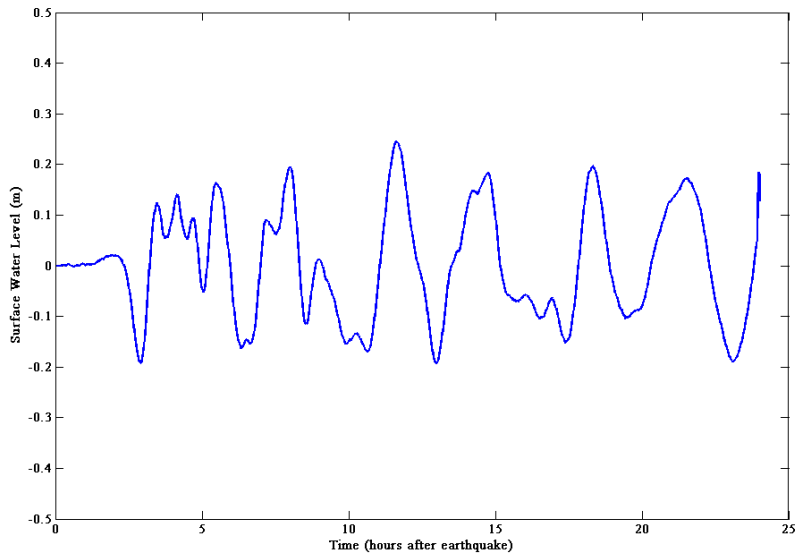
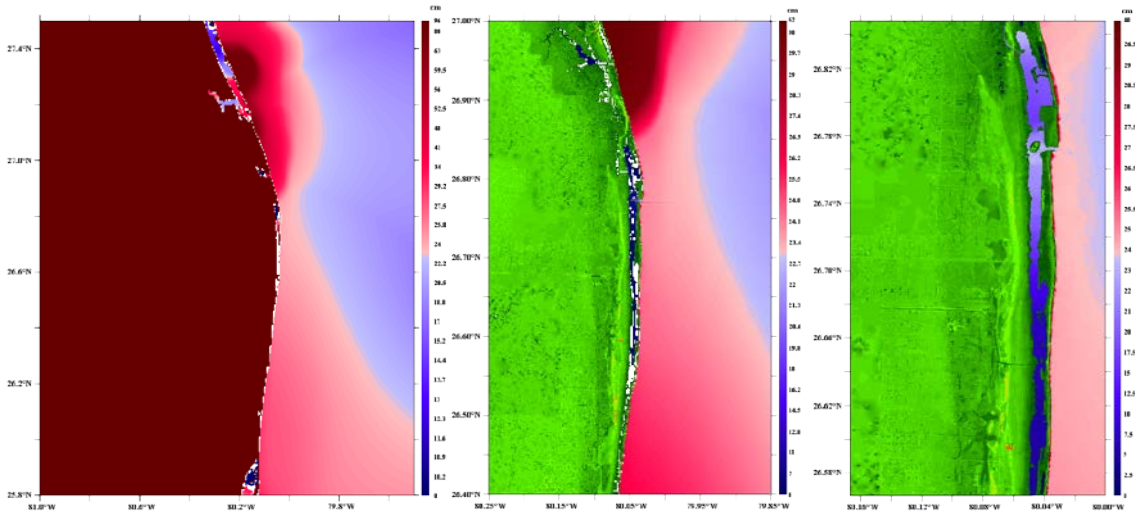


Figure 24. Plot of maximum tsunami wave amplitude distribution [left), A-grid; middle) B-grid and right) C-grid] and time series [bottom) at Lake Worth Pier tide gauge] for mega-event (Mw=9.4) case ATSZ82-91AB using high resolution model.

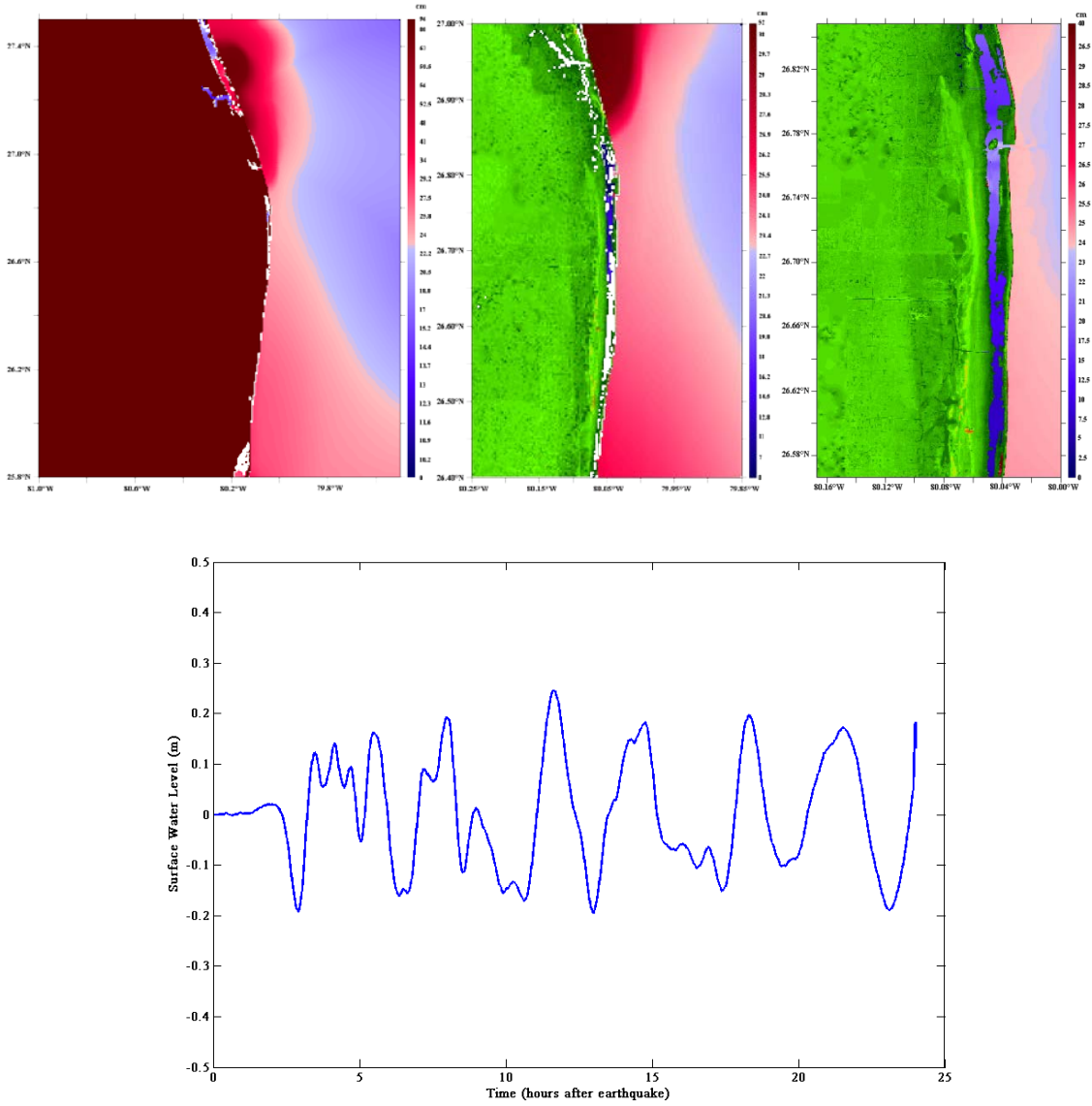


Figure 25. Plot of maximum tsunami wave amplitude distribution [left), A-grid; middle) B-grid and right) C-grid] and time series [bottom) at Lake Worth Pier tide gauge] for mega-event (Mw=9.4) case ATSZ82-91AB using forecast model.

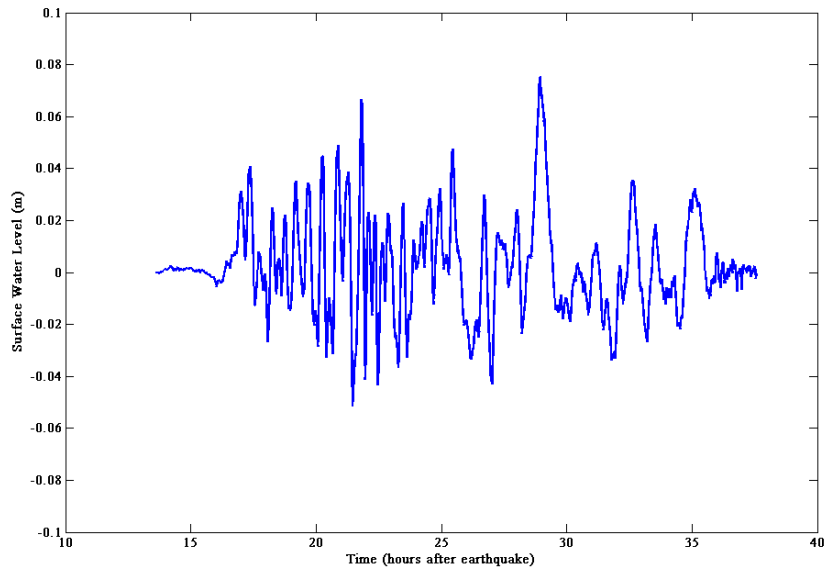
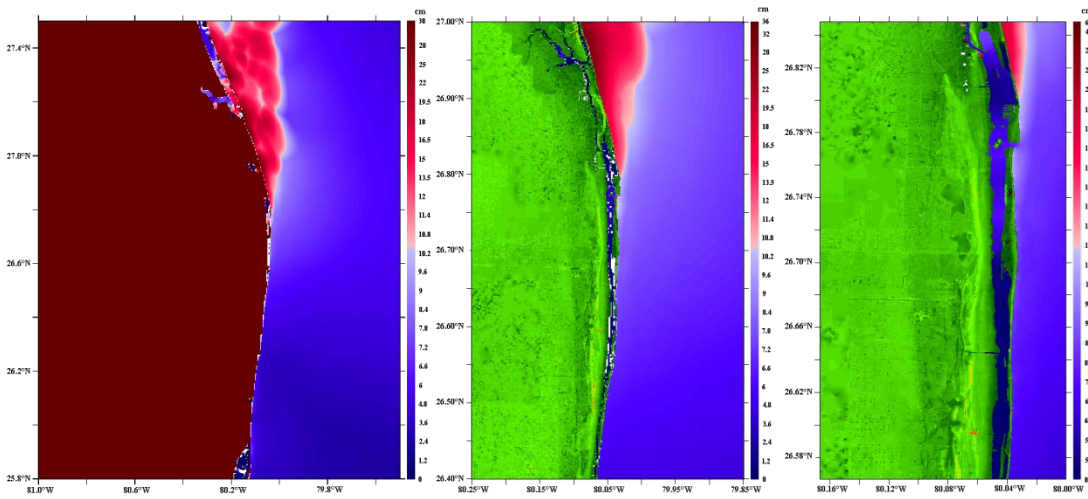


Figure 26. Plot of maximum tsunami wave amplitude distribution [left), A-grid; middle) B-grid and right) C-grid] and time series [bottom) at Lake Worth Pier tide gauge] for mega-event ( $M_w=9.4$ ) case SSSZ01-10AB using high resolution model.

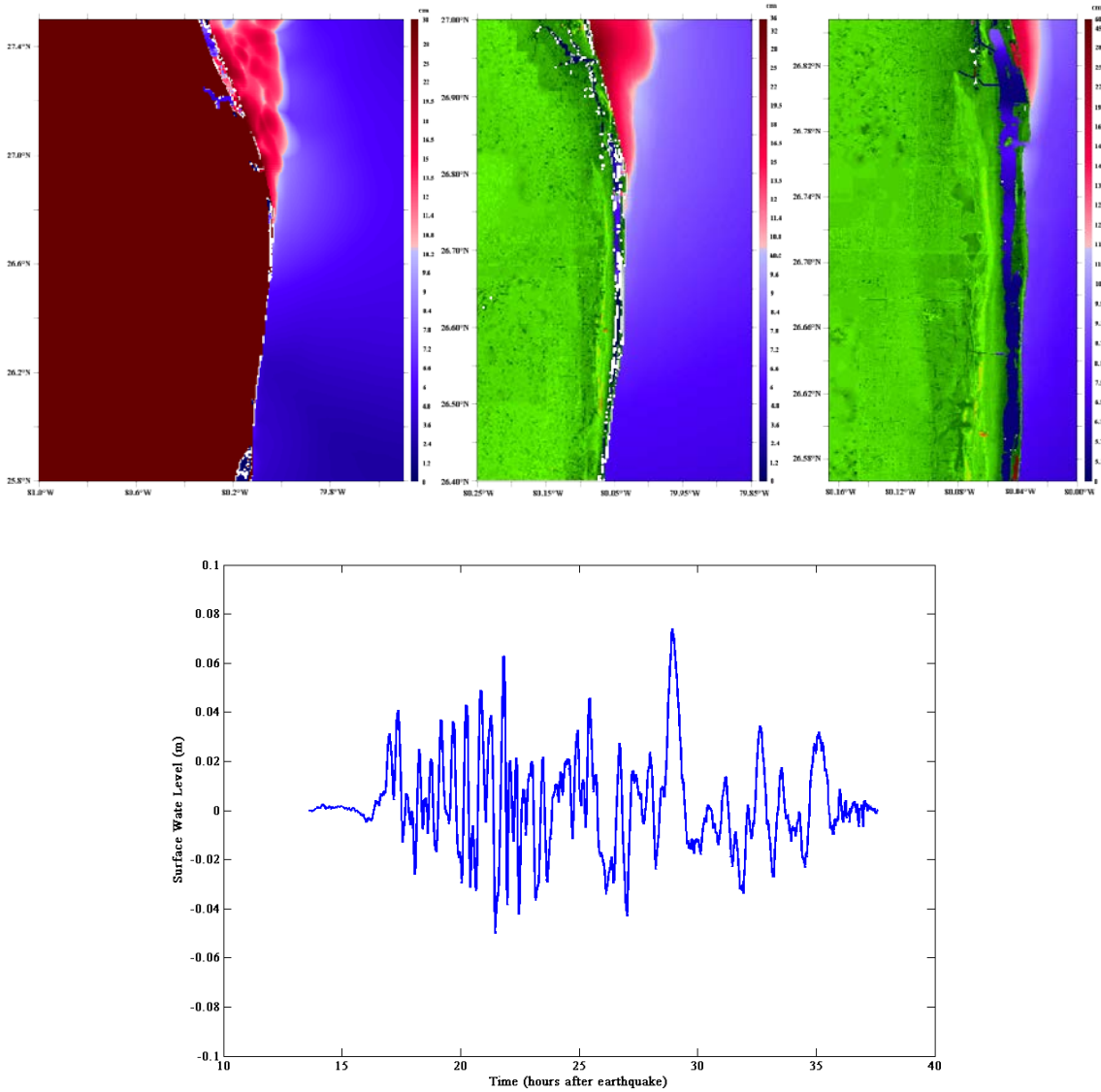


Figure 27. Plot of maximum tsunami wave amplitude distribution [left), A-grid; middle) B-grid and right) C-grid] and time series [bottom) at Lake Worth Pier tide gauge] for mega-event (Mw=9.4) case SSSZ01-10AB using forecast model.



Figure 28. Google map plot of northern part of Singer Island showing the water passage way.

## Appendix A. MOST code \*.in file

Development of the Palm Beach, Florida tsunami forecast model occurred prior to parameter changes that were made to reflect modifications to the MOST model code. As a result, the input file for running both the optimized tsunami forecast model and the high-resolution reference inundation model in MOST have been updated accordingly. Appendix A1 and A2 provide the updated files for Palm Beach, Florida

### A1. Reference model \*.in file for Palm Beach, Florida

0.0001 Minimum amplitude of input offshore wave (m)  
1 Input minimum depth for offshore (m)  
0.1 Input "dry land" depth for inundation (m)  
0.0009 Input friction coefficient ( $n^{*2}$ )  
1 A & B-grid runup flag (0=disallow, 1=allow runup)  
300.0 Blow-up limit (maximum eta before blow-up)  
0.4 Input time step (sec)  
72000 Input number of steps  
5 Compute "A" arrays every  $n^{\text{th}}$  time step,  $n=$   
5 Compute "B" arrays every  $n^{\text{th}}$  time step,  $n=$   
150 Input number of steps between snapshots  
0 ...Starting from  
1 ...Saving grid every  $n^{\text{th}}$  node,  $n=1$

### A2. Forecast model \*.in file for Palm Beach, Florida

0.0001 Minimum amplitude of input offshore wave (m)  
1 Input minimum depth for offshore (m)  
0.1 Input "dry land" depth for inundation (m)  
0.0009 Input friction coefficient ( $n^{*2}$ )  
1 A & B-grid runup flag (0=disallow, 1=allow runup)  
300.0 Blow-up limit (maximum eta before blow-up)  
1.0 Input time step (sec)  
28800 Input number of steps  
4 Compute "A" arrays every  $n^{\text{th}}$  time step,  $n=$   
4 Compute "B" arrays every  $n^{\text{th}}$  time step,  $n=$   
60 Input number of steps between snapshots  
0 ...Starting from  
1 ...Saving grid every  $n^{\text{th}}$  node,  $n=1$

## Appendix B. Propagation Database: Atlantic Ocean Unit Sources

This section lists the earthquake parameters of each unit source in the Atlantic Ocean which covers the Caribbean and South Sandwich sources as of January 30, 2013. The development of the Palm Beach, Florida forecast model was done early 2011 thus using an earlier version of the unit sources.

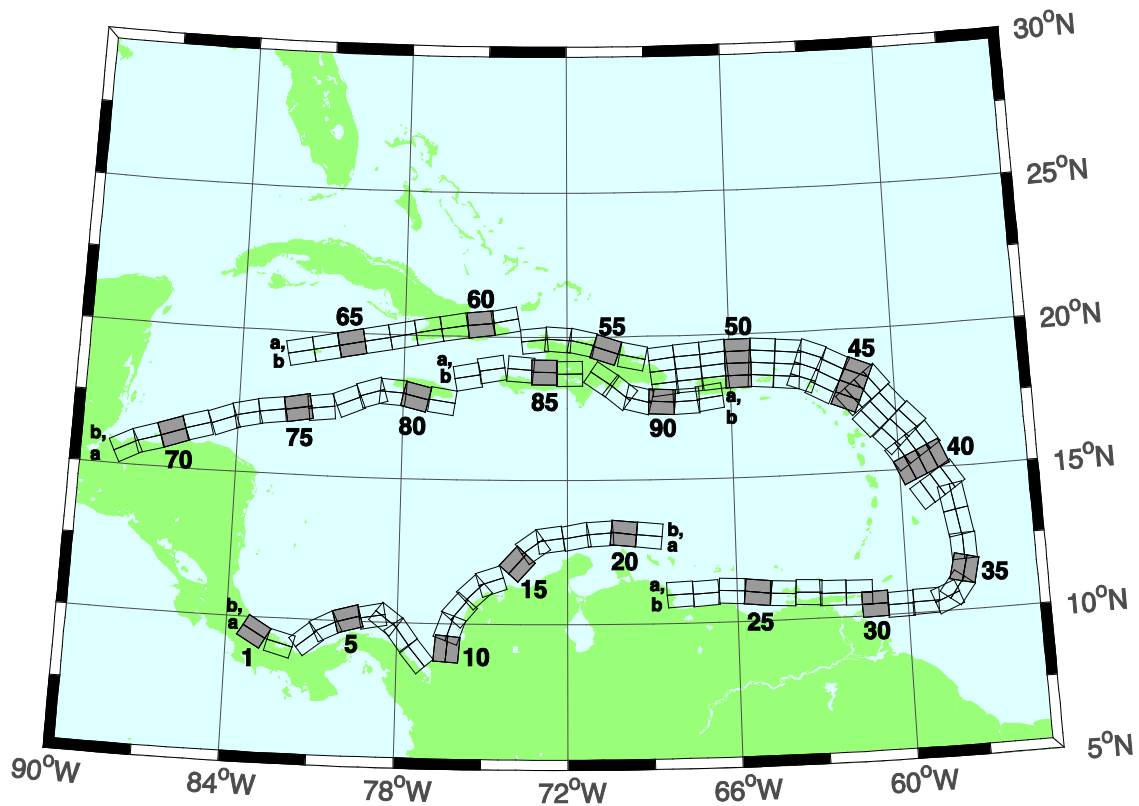


Figure 29. Atlantic Source Zone unit sources

Table 4. Earthquake parameter for unit sources in Atlantic.

Unit Source	Description	Lon (°)	Lat (°)	Strike (°)	Dip (°)	Depth (km)
atsz-01a	Atlantic Source Zone	-83.2020	9.1449	27.50	120.00	28.09
atsz-01b	Atlantic Source Zone	-83.0000	9.4899	27.50	120.00	5.00
atsz-02a	Atlantic Source Zone	-82.1932	8.7408	27.50	105.11	28.09
atsz-02b	Atlantic Source Zone	-82.0880	9.1254	27.50	105.11	5.00
atsz-03a	Atlantic Source Zone	-80.9172	9.0103	30.00	51.31	30.00
atsz-03b	Atlantic Source Zone	-81.1636	9.3139	30.00	51.31	5.00
atsz-04a	Atlantic Source Zone	-80.3265	9.4308	30.00	63.49	30.00
atsz-04b	Atlantic Source Zone	-80.5027	9.7789	30.00	63.49	5.00
atsz-05a	Atlantic Source Zone	-79.6247	9.6961	30.00	74.44	30.00
atsz-05b	Atlantic Source Zone	-79.7307	10.0708	30.00	74.44	5.00
atsz-06a	Atlantic Source Zone	-78.8069	9.8083	30.00	79.71	30.00
atsz-06b	Atlantic Source Zone	-78.8775	10.1910	30.00	79.71	5.00
atsz-07a	Atlantic Source Zone	-78.6237	9.7963	30.00	127.25	30.00
atsz-07b	Atlantic Source Zone	-78.3845	10.1059	30.00	127.25	5.00
atsz-08a	Atlantic Source Zone	-78.1693	9.3544	30.00	143.76	30.00
atsz-08b	Atlantic Source Zone	-77.8511	9.5844	30.00	143.76	5.00
atsz-09a	Atlantic Source Zone	-77.5913	8.5989	30.00	139.93	30.00
atsz-09b	Atlantic Source Zone	-77.2900	8.8493	30.00	139.93	5.00
atsz-10a	Atlantic Source Zone	-75.8109	9.0881	17.00	4.67	19.62
atsz-10b	Atlantic Source Zone	-76.2445	9.1231	17.00	4.67	5.00
atsz-11a	Atlantic Source Zone	-75.7406	9.6929	17.00	19.67	19.62
atsz-11b	Atlantic Source Zone	-76.1511	9.8375	17.00	19.67	5.00
atsz-12a	Atlantic Source Zone	-75.4763	10.2042	17.00	40.40	19.62
atsz-12b	Atlantic Source Zone	-75.8089	10.4826	17.00	40.40	5.00
atsz-13a	Atlantic Source Zone	-74.9914	10.7914	17.00	47.17	19.62
atsz-13b	Atlantic Source Zone	-75.2890	11.1064	17.00	47.17	5.00
atsz-14a	Atlantic Source Zone	-74.5666	11.0708	17.00	71.68	19.62
atsz-14b	Atlantic Source Zone	-74.7043	11.4786	17.00	71.68	5.00
atsz-15a	Atlantic Source Zone	-73.4576	11.8012	17.00	42.69	19.62
atsz-15b	Atlantic Source Zone	-73.7805	12.0924	17.00	42.69	5.00
atsz-16a	Atlantic Source Zone	-72.9788	12.3365	17.00	54.75	19.62
atsz-16b	Atlantic Source Zone	-73.2329	12.6873	17.00	54.75	5.00
atsz-17a	Atlantic Source Zone	-72.5454	12.5061	17.00	81.96	19.62
atsz-17b	Atlantic Source Zone	-72.6071	12.9314	17.00	81.96	5.00
atsz-18a	Atlantic Source Zone	-71.6045	12.6174	17.00	79.63	19.62
atsz-18b	Atlantic Source Zone	-71.6839	13.0399	17.00	79.63	5.00
atsz-19a	Atlantic Source Zone	-70.7970	12.7078	17.00	86.32	19.62
atsz-19b	Atlantic Source Zone	-70.8253	13.1364	17.00	86.32	5.00

Table 4 (continued). Earthquake parameter for unit sources in Atlantic.

atsz-20a	Atlantic Source Zone	-70.0246	12.7185	17.00	95.94	19.62
atsz-20b	Atlantic Source Zone	-69.9789	13.1457	17.00	95.94	5.00
atsz-21a	Atlantic Source Zone	-69.1244	12.6320	17.00	95.94	19.62
atsz-21b	Atlantic Source Zone	-69.0788	13.0592	17.00	95.94	5.00
atsz-22a	Atlantic Source Zone	-68.0338	11.4286	15.00	266.94	17.94
atsz-22b	Atlantic Source Zone	-68.0102	10.9954	15.00	266.94	5.00
atsz-23a	Atlantic Source Zone	-67.1246	11.4487	15.00	266.94	17.94
atsz-23b	Atlantic Source Zone	-67.1010	11.0155	15.00	266.94	5.00
atsz-24a	Atlantic Source Zone	-66.1656	11.5055	15.00	273.30	17.94
atsz-24b	Atlantic Source Zone	-66.1911	11.0724	15.00	273.30	5.00
atsz-25a	Atlantic Source Zone	-65.2126	11.4246	15.00	276.36	17.94
atsz-25b	Atlantic Source Zone	-65.2616	10.9934	15.00	276.36	5.00
atsz-26a	Atlantic Source Zone	-64.3641	11.3516	15.00	272.87	17.94
atsz-26b	Atlantic Source Zone	-64.3862	10.9183	15.00	272.87	5.00
atsz-27a	Atlantic Source Zone	-63.4472	11.3516	15.00	272.93	17.94
atsz-27b	Atlantic Source Zone	-63.4698	10.9183	15.00	272.93	5.00
atsz-28a	Atlantic Source Zone	-62.6104	11.2831	15.00	271.11	17.94
atsz-28b	Atlantic Source Zone	-62.6189	10.8493	15.00	271.11	5.00
atsz-29a	Atlantic Source Zone	-61.6826	11.2518	15.00	271.57	17.94
atsz-29b	Atlantic Source Zone	-61.6947	10.8181	15.00	271.57	5.00
atsz-30a	Atlantic Source Zone	-61.1569	10.8303	15.00	269.01	17.94
atsz-30b	Atlantic Source Zone	-61.1493	10.3965	15.00	269.01	5.00
atsz-31a	Atlantic Source Zone	-60.2529	10.7739	15.00	269.01	17.94
atsz-31b	Atlantic Source Zone	-60.2453	10.3401	15.00	269.01	5.00
atsz-32a	Atlantic Source Zone	-59.3510	10.8123	15.00	269.01	17.94
atsz-32b	Atlantic Source Zone	-59.3734	10.3785	15.00	269.01	5.00
atsz-33a	Atlantic Source Zone	-58.7592	10.8785	15.00	248.62	17.94
atsz-33b	Atlantic Source Zone	-58.5984	10.4745	15.00	248.62	5.00
atsz-34a	Atlantic Source Zone	-58.5699	11.0330	15.00	217.15	17.94
atsz-34b	Atlantic Source Zone	-58.2179	10.7710	15.00	217.15	5.00
atsz-35a	Atlantic Source Zone	-58.3549	11.5300	15.00	193.68	17.94
atsz-35b	Atlantic Source Zone	-57.9248	11.4274	15.00	193.68	5.00
atsz-36a	Atlantic Source Zone	-58.3432	12.1858	15.00	177.65	17.94
atsz-36b	Atlantic Source Zone	-57.8997	12.2036	15.00	177.65	5.00
atsz-37a	Atlantic Source Zone	-58.4490	12.9725	15.00	170.73	17.94
atsz-37b	Atlantic Source Zone	-58.0095	13.0424	15.00	170.73	5.00
atsz-38a	Atlantic Source Zone	-58.6079	13.8503	15.00	170.22	17.94
atsz-38b	Atlantic Source Zone	-58.1674	13.9240	15.00	170.22	5.00
atsz-39a	Atlantic Source Zone	-58.6667	14.3915	15.00	146.85	17.94
atsz-39b	Atlantic Source Zone	-58.2913	14.6287	15.00	146.85	5.00

Table 4 (continued). Earthquake parameter for unit sources in Atlantic.

atsz-39y	Atlantic Source Zone	-59.4168	13.9171	15.00	146.85	43.82
atsz-39z	Atlantic Source Zone	-59.0415	14.1543	15.00	146.85	30.88
atsz-40a	Atlantic Source Zone	-59.1899	15.2143	15.00	156.23	17.94
atsz-40b	Atlantic Source Zone	-58.7781	15.3892	15.00	156.23	5.00
atsz-40y	Atlantic Source Zone	-60.0131	14.8646	15.00	156.23	43.82
atsz-40z	Atlantic Source Zone	-59.6012	15.0395	15.00	156.23	30.88
atsz-41a	Atlantic Source Zone	-59.4723	15.7987	15.00	146.33	17.94
atsz-41b	Atlantic Source Zone	-59.0966	16.0392	15.00	146.33	5.00
atsz-41y	Atlantic Source Zone	-60.2229	15.3177	15.00	146.33	43.82
atsz-41z	Atlantic Source Zone	-59.8473	15.5582	15.00	146.33	30.88
atsz-42a	Atlantic Source Zone	-59.9029	16.4535	15.00	136.99	17.94
atsz-42b	Atlantic Source Zone	-59.5716	16.7494	15.00	136.99	5.00
atsz-42y	Atlantic Source Zone	-60.5645	15.8616	15.00	136.99	43.82
atsz-42z	Atlantic Source Zone	-60.2334	16.1575	15.00	136.99	30.88
atsz-43a	Atlantic Source Zone	-60.5996	17.0903	15.00	138.71	17.94
atsz-43b	Atlantic Source Zone	-60.2580	17.3766	15.00	138.71	5.00
atsz-43y	Atlantic Source Zone	-61.2818	16.5177	15.00	138.71	43.82
atsz-43z	Atlantic Source Zone	-60.9404	16.8040	15.00	138.71	30.88
atsz-44a	Atlantic Source Zone	-61.1559	17.8560	15.00	141.07	17.94
atsz-44b	Atlantic Source Zone	-60.8008	18.1286	15.00	141.07	5.00
atsz-44y	Atlantic Source Zone	-61.8651	17.3108	15.00	141.07	43.82
atsz-44z	Atlantic Source Zone	-61.5102	17.5834	15.00	141.07	30.88
atsz-45a	Atlantic Source Zone	-61.5491	18.0566	15.00	112.84	17.94
atsz-45b	Atlantic Source Zone	-61.3716	18.4564	15.00	112.84	5.00
atsz-45y	Atlantic Source Zone	-61.9037	17.2569	15.00	112.84	43.82
atsz-45z	Atlantic Source Zone	-61.7260	17.6567	15.00	112.84	30.88
atsz-46a	Atlantic Source Zone	-62.4217	18.4149	15.00	117.86	17.94
atsz-46b	Atlantic Source Zone	-62.2075	18.7985	15.00	117.86	5.00
atsz-46y	Atlantic Source Zone	-62.8493	17.6477	15.00	117.86	43.82
atsz-46z	Atlantic Source Zone	-62.6352	18.0313	15.00	117.86	30.88
atsz-47a	Atlantic Source Zone	-63.1649	18.7844	20.00	110.46	22.10
atsz-47b	Atlantic Source Zone	-63.0087	19.1798	20.00	110.46	5.00
atsz-47y	Atlantic Source Zone	-63.4770	17.9936	20.00	110.46	56.30
atsz-47z	Atlantic Source Zone	-63.3205	18.3890	20.00	110.46	39.20
atsz-48a	Atlantic Source Zone	-63.8800	18.8870	20.00	95.37	22.10
atsz-48b	Atlantic Source Zone	-63.8382	19.3072	20.00	95.37	5.00
atsz-48y	Atlantic Source Zone	-63.9643	18.0465	20.00	95.37	56.30
atsz-48z	Atlantic Source Zone	-63.9216	18.4667	20.00	95.37	39.20
atsz-49a	Atlantic Source Zone	-64.8153	18.9650	20.00	94.34	22.10
atsz-49b	Atlantic Source Zone	-64.7814	19.3859	20.00	94.34	5.00

Table 4 (continued). Earthquake parameter for unit sources in Atlantic.

atsz-49y	Atlantic Source Zone	-64.8840	18.1233	20.00	94.34	56.30
atsz-49z	Atlantic Source Zone	-64.8492	18.5442	20.00	94.34	39.20
atsz-50a	Atlantic Source Zone	-65.6921	18.9848	20.00	89.59	22.10
atsz-50b	Atlantic Source Zone	-65.6953	19.4069	20.00	89.59	5.00
atsz-50y	Atlantic Source Zone	-65.6874	18.1407	20.00	89.59	56.30
atsz-50z	Atlantic Source Zone	-65.6887	18.5628	20.00	89.59	39.20
atsz-51a	Atlantic Source Zone	-66.5742	18.9484	20.00	84.98	22.10
atsz-51b	Atlantic Source Zone	-66.6133	19.3688	20.00	84.98	5.00
atsz-51y	Atlantic Source Zone	-66.4977	18.1076	20.00	84.98	56.30
atsz-51z	Atlantic Source Zone	-66.5353	18.5280	20.00	84.98	39.20
atsz-52a	Atlantic Source Zone	-67.5412	18.8738	20.00	85.87	22.10
atsz-52b	Atlantic Source Zone	-67.5734	19.2948	20.00	85.87	5.00
atsz-52y	Atlantic Source Zone	-67.4781	18.0319	20.00	85.87	56.30
atsz-52z	Atlantic Source Zone	-67.5090	18.4529	20.00	85.87	39.20
atsz-53a	Atlantic Source Zone	-68.4547	18.7853	20.00	83.64	22.10
atsz-53b	Atlantic Source Zone	-68.5042	19.2048	20.00	83.64	5.00
atsz-53y	Atlantic Source Zone	-68.3575	17.9463	20.00	83.64	56.30
atsz-53z	Atlantic Source Zone	-68.4055	18.3658	20.00	83.64	39.20
atsz-54a	Atlantic Source Zone	-69.6740	18.8841	20.00	101.54	22.10
atsz-54b	Atlantic Source Zone	-69.5846	19.2976	20.00	101.54	5.00
atsz-55a	Atlantic Source Zone	-70.7045	19.1376	20.00	108.19	22.10
atsz-55b	Atlantic Source Zone	-70.5647	19.5386	20.00	108.19	5.00
atsz-56a	Atlantic Source Zone	-71.5368	19.3853	20.00	102.64	22.10
atsz-56b	Atlantic Source Zone	-71.4386	19.7971	20.00	102.64	5.00
atsz-57a	Atlantic Source Zone	-72.3535	19.4838	20.00	94.20	22.10
atsz-57b	Atlantic Source Zone	-72.3206	19.9047	20.00	94.20	5.00
atsz-58a	Atlantic Source Zone	-73.1580	19.4498	20.00	84.34	22.10
atsz-58b	Atlantic Source Zone	-73.2022	19.8698	20.00	84.34	5.00
atsz-59a	Atlantic Source Zone	-74.3567	20.9620	20.00	259.74	22.10
atsz-59b	Atlantic Source Zone	-74.2764	20.5467	20.00	259.74	5.00
atsz-60a	Atlantic Source Zone	-75.2386	20.8622	15.00	264.18	17.94
atsz-60b	Atlantic Source Zone	-75.1917	20.4306	15.00	264.18	5.00
atsz-61a	Atlantic Source Zone	-76.2383	20.7425	15.00	260.70	17.94
atsz-61b	Atlantic Source Zone	-76.1635	20.3144	15.00	260.70	5.00
atsz-62a	Atlantic Source Zone	-77.2021	20.5910	15.00	259.95	17.94
atsz-62b	Atlantic Source Zone	-77.1214	20.1638	15.00	259.95	5.00
atsz-63a	Atlantic Source Zone	-78.1540	20.4189	15.00	259.03	17.94
atsz-63b	Atlantic Source Zone	-78.0661	19.9930	15.00	259.03	5.00
atsz-64a	Atlantic Source Zone	-79.0959	20.2498	15.00	259.24	17.94
atsz-64b	Atlantic Source Zone	-79.0098	19.8236	15.00	259.24	5.00

Table 4 (continued). Earthquake parameter for unit sources in Atlantic.

atsz-65a	Atlantic Source Zone	-80.0393	20.0773	15.00	258.85	17.94
atsz-65b	Atlantic Source Zone	-79.9502	19.6516	15.00	258.85	5.00
atsz-66a	Atlantic Source Zone	-80.9675	19.8993	15.00	258.60	17.94
atsz-66b	Atlantic Source Zone	-80.8766	19.4740	15.00	258.60	5.00
atsz-67a	Atlantic Source Zone	-81.9065	19.7214	15.00	258.51	17.94
atsz-67b	Atlantic Source Zone	-81.8149	19.2962	15.00	258.51	5.00
atsz-68a	Atlantic Source Zone	-87.8003	15.2509	15.00	62.69	17.94
atsz-68b	Atlantic Source Zone	-88.0070	15.6364	15.00	62.69	5.00
atsz-69a	Atlantic Source Zone	-87.0824	15.5331	15.00	72.73	17.94
atsz-69b	Atlantic Source Zone	-87.2163	15.9474	15.00	72.73	5.00
atsz-70a	Atlantic Source Zone	-86.1622	15.8274	15.00	70.64	17.94
atsz-70b	Atlantic Source Zone	-86.3120	16.2367	15.00	70.64	5.00
atsz-71a	Atlantic Source Zone	-85.3117	16.1052	15.00	73.70	17.94
atsz-71b	Atlantic Source Zone	-85.4387	16.5216	15.00	73.70	5.00
atsz-72a	Atlantic Source Zone	-84.3470	16.3820	15.00	69.66	17.94
atsz-72b	Atlantic Source Zone	-84.5045	16.7888	15.00	69.66	5.00
atsz-73a	Atlantic Source Zone	-83.5657	16.6196	15.00	77.36	17.94
atsz-73b	Atlantic Source Zone	-83.6650	17.0429	15.00	77.36	5.00
atsz-74a	Atlantic Source Zone	-82.7104	16.7695	15.00	82.35	17.94
atsz-74b	Atlantic Source Zone	-82.7709	17.1995	15.00	82.35	5.00
atsz-75a	Atlantic Source Zone	-81.7297	16.9003	15.00	79.86	17.94
atsz-75b	Atlantic Source Zone	-81.8097	17.3274	15.00	79.86	5.00
atsz-76a	Atlantic Source Zone	-80.9196	16.9495	15.00	82.95	17.94
atsz-76b	Atlantic Source Zone	-80.9754	17.3801	15.00	82.95	5.00
atsz-77a	Atlantic Source Zone	-79.8086	17.2357	15.00	67.95	17.94
atsz-77b	Atlantic Source Zone	-79.9795	17.6378	15.00	67.95	5.00
atsz-78a	Atlantic Source Zone	-79.0245	17.5415	15.00	73.61	17.94
atsz-78b	Atlantic Source Zone	-79.1532	17.9577	15.00	73.61	5.00
atsz-79a	Atlantic Source Zone	-78.4122	17.5689	15.00	94.07	17.94
atsz-79b	Atlantic Source Zone	-78.3798	18.0017	15.00	94.07	5.00
atsz-80a	Atlantic Source Zone	-77.6403	17.4391	15.00	103.33	17.94
atsz-80b	Atlantic Source Zone	-77.5352	17.8613	15.00	103.33	5.00
atsz-81a	Atlantic Source Zone	-76.6376	17.2984	15.00	98.21	17.94
atsz-81b	Atlantic Source Zone	-76.5726	17.7278	15.00	98.21	5.00
atsz-82a	Atlantic Source Zone	-75.7299	19.0217	15.00	260.15	17.94
atsz-82b	Atlantic Source Zone	-75.6516	18.5942	15.00	260.15	5.00
atsz-83a	Atlantic Source Zone	-74.8351	19.2911	15.00	260.83	17.94
atsz-83b	Atlantic Source Zone	-74.7621	18.8628	15.00	260.83	5.00
atsz-84a	Atlantic Source Zone	-73.6639	19.2991	15.00	274.84	17.94
atsz-84b	Atlantic Source Zone	-73.7026	18.8668	15.00	274.84	5.00

Table 4 (continued). Earthquake parameter for unit sources in Atlantic.

atsz-85a	Atlantic Source Zone	-72.8198	19.2019	15.00	270.60	17.94
atsz-85b	Atlantic Source Zone	-72.8246	18.7681	15.00	270.60	5.00
atsz-86a	Atlantic Source Zone	-71.9143	19.1477	15.00	269.06	17.94
atsz-86b	Atlantic Source Zone	-71.9068	18.7139	15.00	269.06	5.00
atsz-87a	Atlantic Source Zone	-70.4738	18.8821	15.00	304.49	17.94
atsz-87b	Atlantic Source Zone	-70.7329	18.5245	15.00	304.49	5.00
atsz-88a	Atlantic Source Zone	-69.7710	18.3902	15.00	308.94	17.94
atsz-88b	Atlantic Source Zone	-70.0547	18.0504	15.00	308.44	5.00
atsz-89a	Atlantic Source Zone	-69.2635	18.2099	15.00	283.88	17.94
atsz-89b	Atlantic Source Zone	-69.3728	17.7887	15.00	283.88	5.00
atsz-90a	Atlantic Source Zone	-68.5059	18.1443	15.00	272.93	17.94
atsz-90b	Atlantic Source Zone	-68.5284	17.7110	15.00	272.93	5.00
atsz-91a	Atlantic Source Zone	-67.6428	18.1438	15.00	267.84	17.94
atsz-91b	Atlantic Source Zone	-67.6256	17.7103	15.00	267.84	5.00
atsz-92a	Atlantic Source Zone	-66.8261	18.2536	15.00	262.00	17.94
atsz-92b	Atlantic Source Zone	-66.7627	17.8240	15.00	262.00	5.00

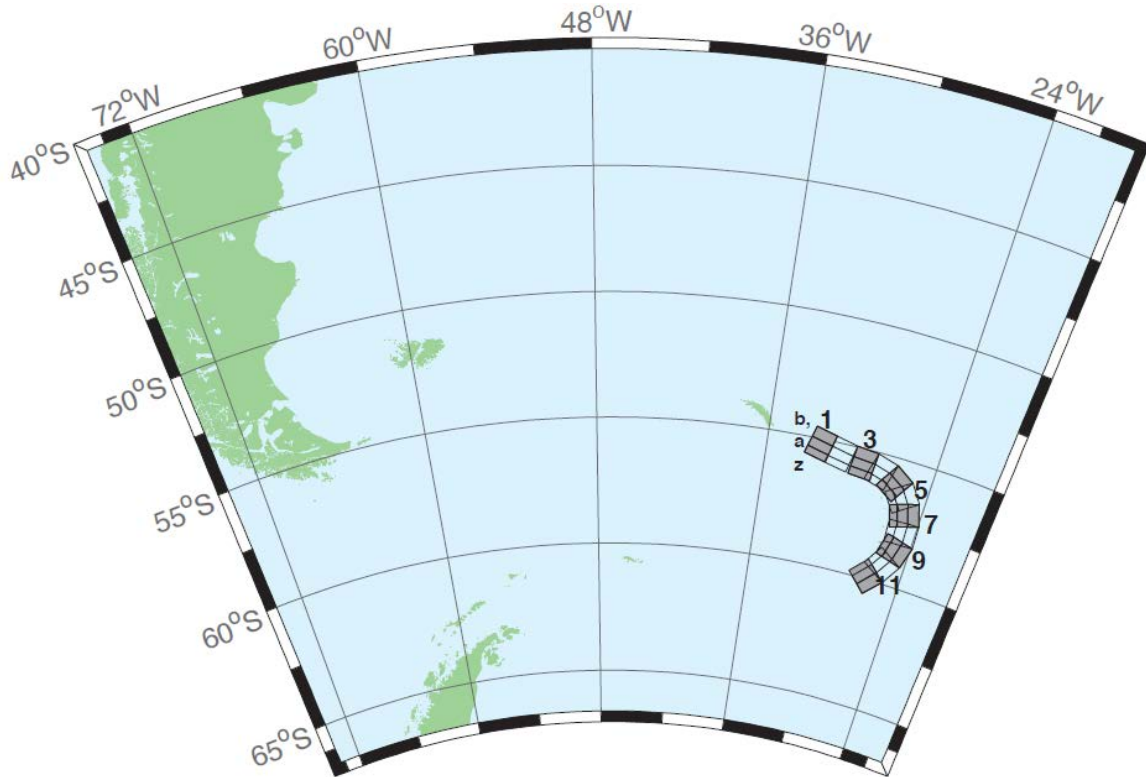


Figure 30. South Sandwich Source Zone unit sources

Table 5. Earthquake parameters for unit sources in South Sandwich.

sssz-01a	South Sandwich Source Zone	-32.3713	-55.4655	28.528	104.6905	17.511
sssz-01b	South Sandwich Source Zone	-32.1953	-55.0832	9.957	104.6905	8.866
sssz-01z	South Sandwich Source Zone	-32.5091	-55.7624	46.989	104.6905	41.391
sssz-02a	South Sandwich Source Zone	-30.8028	-55.6842	28.528	102.4495	17.511
sssz-02b	South Sandwich Source Zone	-30.6524	-55.2982	9.957	102.4495	8.866
sssz-02z	South Sandwich Source Zone	-30.9207	-55.9839	46.989	102.4495	41.391
sssz-03a	South Sandwich Source Zone	-29.0824	-55.8403	28.528	95.5322	17.511
sssz-03b	South Sandwich Source Zone	-29.0149	-55.4469	9.957	95.5322	8.866
sssz-03z	South Sandwich Source Zone	-29.1354	-56.1458	46.989	95.5322	41.391
sssz-04a	South Sandwich Source Zone	-27.8128	-55.9796	28.528	106.1387	17.511
sssz-04b	South Sandwich Source Zone	-27.6174	-55.5999	9.957	106.1387	8.866
sssz-04z	South Sandwich Source Zone	-27.9659	-56.2744	46.989	106.1387	41.391
sssz-05a	South Sandwich Source Zone	-26.7928	-56.2481	28.528	123.1030	17.511
sssz-05b	South Sandwich Source Zone	-26.4059	-55.9170	9.957	123.1030	8.866
sssz-05z	South Sandwich Source Zone	-27.0955	-56.5052	46.989	123.1030	41.391
sssz-06a	South Sandwich Source Zone	-26.1317	-56.6466	23.277	145.6243	16.110
sssz-06b	South Sandwich Source Zone	-25.5131	-56.4133	9.090	145.6243	8.228
sssz-06z	South Sandwich Source Zone	-26.5920	-56.8194	47.151	145.6243	35.869
sssz-07a	South Sandwich Source Zone	-25.6787	-57.2162	21.210	162.9420	14.235
sssz-07b	South Sandwich Source Zone	-24.9394	-57.0932	7.596	162.9420	7.626
sssz-07z	South Sandwich Source Zone	-26.2493	-57.3109	44.159	162.9420	32.324
sssz-08a	South Sandwich Source Zone	-25.5161	-57.8712	20.328	178.2111	15.908
sssz-08b	South Sandwich Source Zone	-24.7233	-57.8580	8.449	178.2111	8.562
sssz-08z	South Sandwich Source Zone	-26.1280	-57.8813	43.649	178.2111	33.278
sssz-09a	South Sandwich Source Zone	-25.6657	-58.5053	25.759	195.3813	15.715
sssz-09b	South Sandwich Source Zone	-24.9168	-58.6128	8.254	195.3813	8.537
sssz-09z	South Sandwich Source Zone	-26.1799	-58.4313	51.691	195.3813	37.444
sssz-10a	South Sandwich Source Zone	-26.1563	-59.1048	32.821	212.5129	15.649
sssz-10b	South Sandwich Source Zone	-25.5335	-59.3080	10.449	212.5129	6.581
sssz-10z	South Sandwich Source Zone	-26.5817	-58.9653	54.773	212.5129	42.750
sssz-11a	South Sandwich Source Zone	-27.0794	-59.6799	33.667	224.2397	15.746
sssz-11b	South Sandwich Source Zone	-26.5460	-59.9412	11.325	224.2397	5.927
sssz-11z	South Sandwich Source Zone	-27.4245	-59.5098	57.190	224.2397	43.464

## **Appendix C. Forecast Model tests in SIFT system.**

The development of the Forecast models requires that it can provide a reliable and stable for several hours of simulation. This is accomplished by testing the forecast model with a set of synthetic tsunami events covering a range of tsunami source locations and magnitudes. Testing is also done with selected historical tsunami events when available.

The purpose of testing the forecast model using the Desktop SIFT system is three-fold. The first objective is to assure that the results obtained with NOAA's tsunami forecast system (SIFT system), which has been released to the Tsunami Warning Centers for operational use, are similar to those obtained by the researcher during the development of the forecast model. The second objective is to test the forecast model for consistency, accuracy, time efficiency, and quality of results over a range of possible tsunami locations and magnitudes. The third objective is to identify bugs and issues in need of resolution by the researcher who developed the Forecast Model or by the forecast software development team before the next version release to NOAA's two Tsunami Warning Centers.

Local hardware and software applications, and tools familiar to the researcher(s), are used to run the Method of Splitting Tsunamis (MOST) model during the forecast model development. The test results presented in this section lend confidence that the model performs as developed and produces the same results when initiated within the forecast application in an operational setting as those produced by the researcher during the forecast model development. The test results assure those who rely on the Palm Beach, Florida tsunami forecast model that consistent results are produced irrespective of system.

### **C.1 Testing Procedure**

The general procedure for forecast model testing is to run a set of synthetic tsunami scenarios and a selected set of historical tsunami events through the forecast system application and compare the results with those obtained by the researcher during the forecast model development as presented in the Tsunami Forecast Model Report. Specific steps taken to test the model include:

1. Identification of testing scenarios, including the standard set of synthetic events, appropriate historical events, and customized synthetic scenarios that may have been used by the researcher(s) in developing the forecast model.
2. Creation of new events to represent customized synthetic scenarios used by the researcher(s) in developing the forecast model, if any.
3. Submission of test model runs with the forecast system, and export of the results from A, B, and C grids, along with time series.
4. Recording applicable metadata, including the specific version of the forecast system used for testing.
5. Examination of forecast model results for instabilities in both time series and plot results.
6. Comparison of forecast model results obtained through the forecast system with those obtained during the forecast model development.
7. Summarization of results with specific mention of quality, consistency, and time efficiency.
8. Reporting of issues identified to modeler and forecast software development team.
9. Retesting the forecast models in the forecast system when reported issues have been address or explained.

Simulation of the Synthetic model were tested on a DELL PowerEdge R510 computer equipped with two Xeon E5670 processors at 2.93 GHz, each with 12 MBytes of cache and 32GB memory. The processors are hex core and support hyper-threading, resulting in the computer performing as a 24 processor core machine. Additionally, the testing computer supports 10 Gigabit Ethernet for fast network connections. This computer configuration is similar or the same as the configurations of the computers installed at the Tsunami Warning Centers so the compute times should only vary slightly

## **C.2 Results**

The Palm Beach, Florida forecast model was tested with NOAA's tsunami forecast system version 3.2.

The Palm Beach, Florida forecast model was tested with three synthetic scenarios. Test results from the forecast system and comparisons with the results obtained during the forecast model development are shown numerically in Table 6 and graphically in Figures 31 to 33. The results show that the forecast model is stable and robust, with consistent and high quality results across geographically distributed tsunami sources. The model run time (wall clock time) was 22.62 minutes for 7.99 hours of simulation time, and 11.32

minutes for 4.0 hours. This run time is not within the 10 minute run time for 4 hours of simulation time and does not satisfy time efficiency requirements. The trade-off for taking more than 10 minutes to simulate 4 hours of tsunami waves is the grid resolution used and the coverage extent of the forecast model at C-grid level. Satisfying a 10-minute run would require a smaller coverage of the C-grid level or a coarser grid resolution or a combination of both.

A suite of three synthetic events was run on the Palm Beach, Florida forecast model. The modeled scenarios were stable for all cases tested, with no instabilities or ringing. The standard 25 meter slip was not used for synthetic cases during development; instead a 30 meter slip was used. Therefore, a 30 meter slip was used for direct comparison purposes. The largest modeled height was 95 centimeters (cm) and originated from the Atlantic (ATSZ48-57) source. The smallest signal of 2.8 cm originated from the South Sandwich (SSSZ01-10) source. Direct comparisons of output from the forecast tool with development results demonstrated that the wave pattern were similar in shape, pattern and amplitude. Both the maximum and minimum amplitudes obtained during forecast model development of Palm Beach were higher than the maximum amplitudes obtained using the tsunami forecast software. The most significant being a 13.2 cm difference for the ATSZ48-57 for the maximum amplitude and 8.1 cm for the minimum amplitude with scenario ATSZ38-47. This difference is attributed to the updates done on the Atlantic Source Zone unit sources. The updates on the unit source were done sometime after the Palm Beach, Florida forecast model was developed.

Table 6. Table of maximum and minimum amplitudes (cm) at the Palm Beach, Florida warning point for synthetic and historical events tested using SIFT 3.2 and obtained during development.

<b>Scenario Name</b>	<b>Source Zone</b>	<b>Tsunami Source</b>	<b><math>\alpha</math> [m]</b>	<b>SIFT Max (cm)</b>	<b>Development Max (cm)</b>	<b>SIFT Min (cm)</b>	<b>Development Min (cm)</b>
<b>Mega-tsunami Scenarios</b>							
ATSZ 38-47	Atlantic	A38-A47, B38-B47	30	22.9	24.2	-14.4	-22.5
ATSZ 48-57	Atlantic	A48-A57, B48-B57	30	95.0	108.2	-89.2	-92.1
SSSZ 01-10	South Sandwich	A01-A10, B1-B10	30	2.8	7.4	-2.0	-5.0

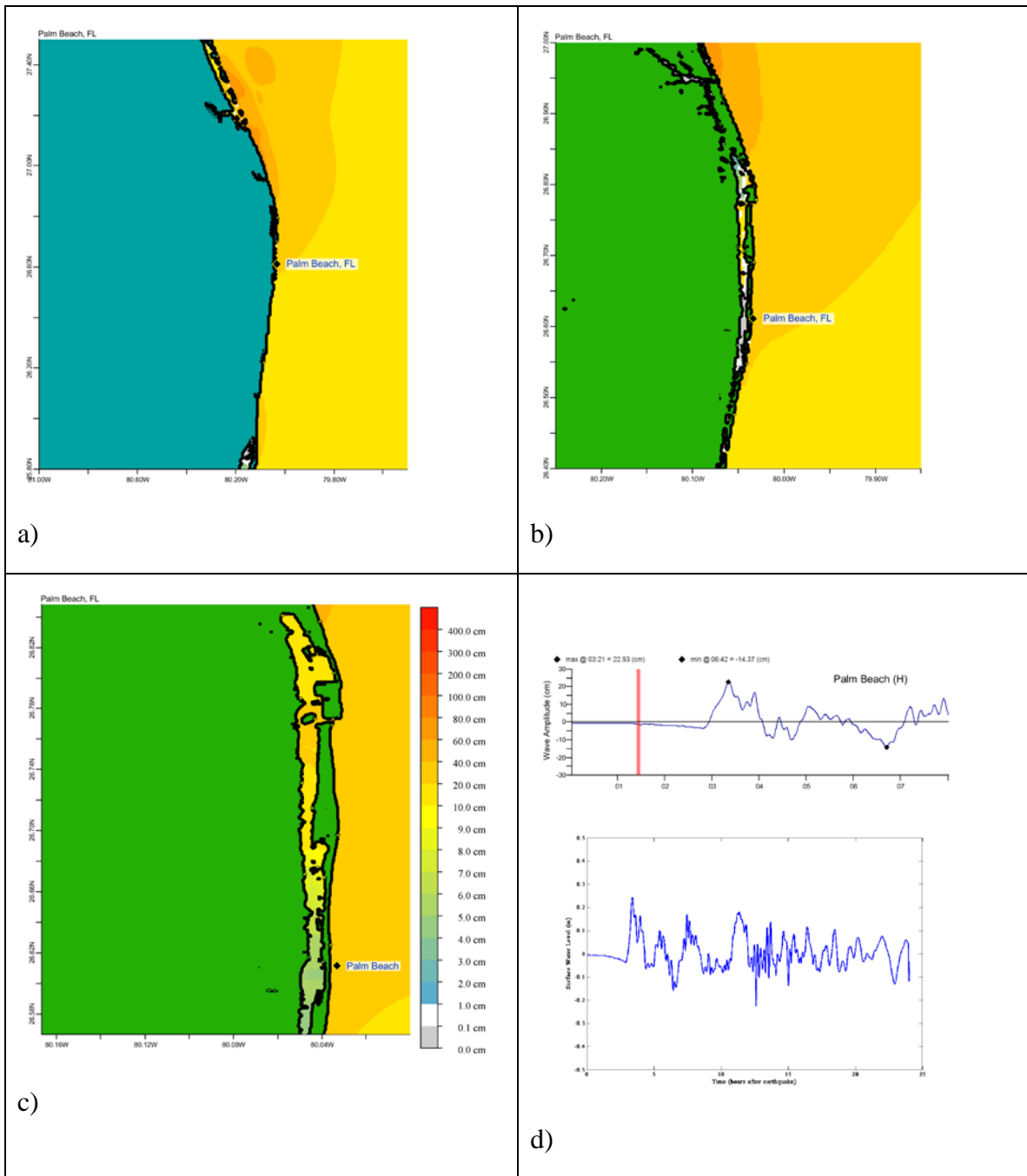


Figure 31. Response of the Palm Beach forecast model to synthetic scenario ATSZ 38-47 ( $\alpha=30$ ). Maximum sea surface elevation for a) A-grid, b) B-grid, c) C-grid. Sea surface elevation time series at the C-grid warning point (d). The lower time series plot is the result obtained during model development and is shown for comparison with test results.

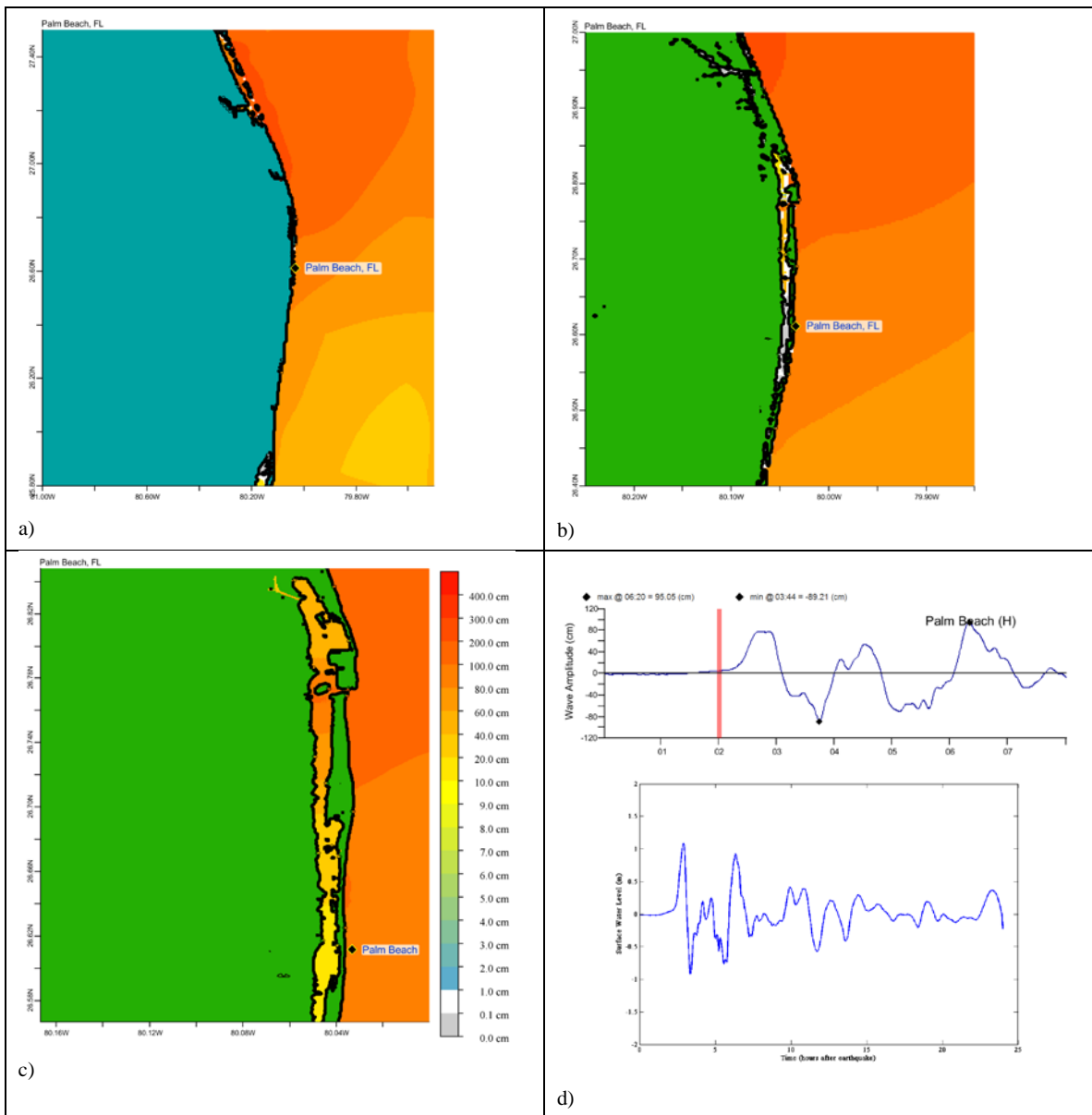


Figure 32 Response of the Palm Beach forecast model to synthetic scenario ATSZ 48-57 ( $\alpha=30$ ). Maximum sea surface elevation for a) A-grid, b) B-grid, c) C-grid. Sea surface elevation time series at the C-grid warning point (d). The lower time series plot is the result obtained during model development and is shown for comparison with test results.

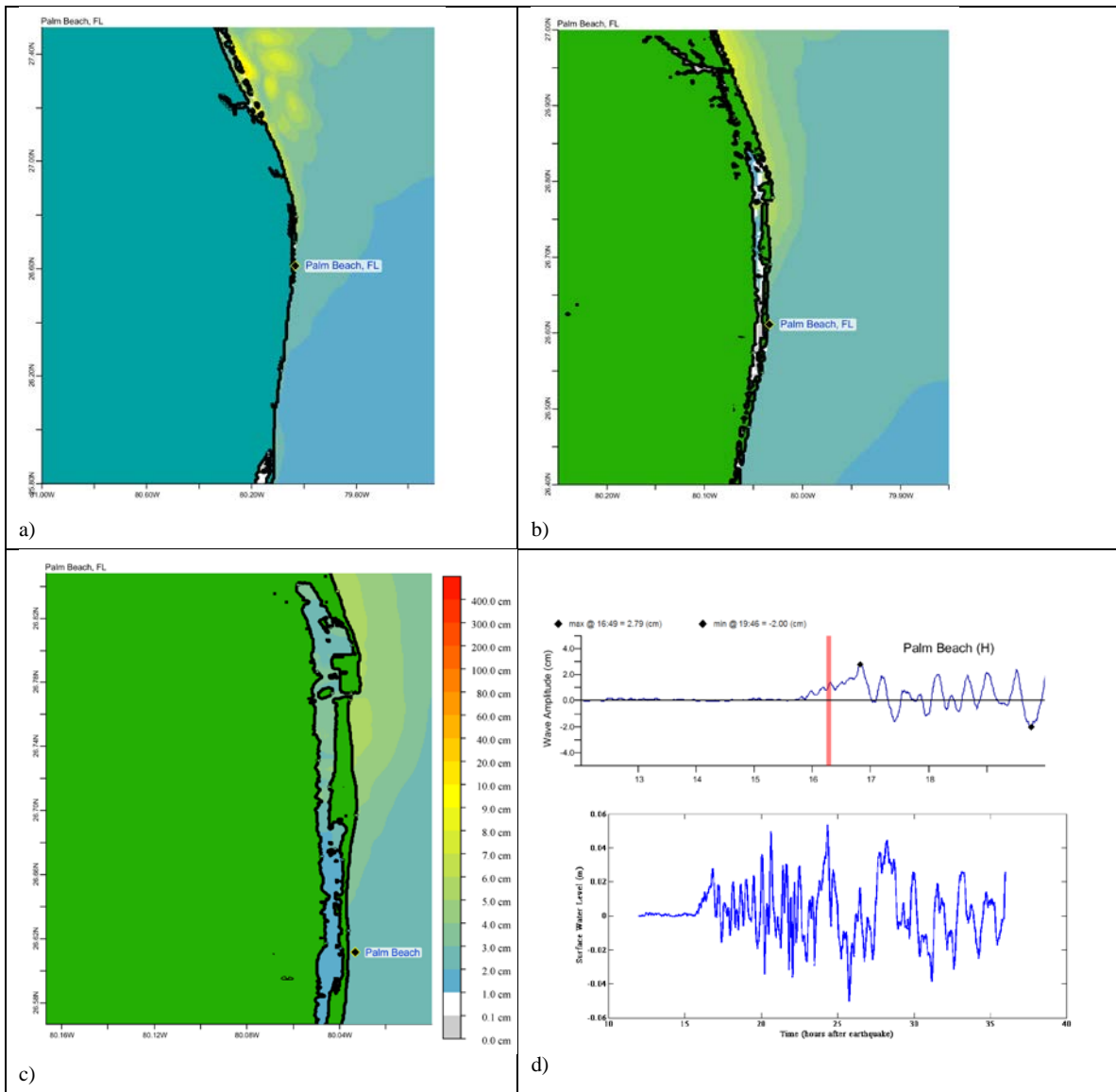


Figure 33. Response of the Palm Beach forecast model to synthetic scenario SSSZ 01-10 (alpha=30). Maximum sea surface elevation for (a) A-grid, b) B-grid, c) C-grid. Sea surface elevation time series at the C-grid warning point (d). The lower time series plot is the result obtained during model development and is shown for comparison with test results.